Bar Ilan University

Optimization of Transmitting and Receiving Coils for Improved Energy Transfer Efficiency in Dynamic Wireless Electric Vehicle Charging systems

Itay Garrofy

Submitted in partial fulfillment of the requirements of the Master's Degree in the Department of Physics, Bar Ilan University

Ramat Gan, Israel 2025

This work was carried out under the supervision of

Dr. Shuki Wolfus

Department of Physics, Bar-Ilan University.

Table of Contents

Abstract

The growing demand for sustainable energy solutions has significantly driven the adoption of electric vehicles (EVs), underscoring the need for innovative and efficient charging technologies. Conventional charging methods, reliant on stationary points and prolonged durations, pose challenges to the operational efficiency and range of EVs. Dynamic Wireless Power Transfer (DWPT) emerges as a transformative approach, enabling continuous energy transfer from road-embedded transmitter coils to vehicle-mounted receiver coils, thereby allowing EVs to charge seamlessly while in motion. This research focuses on optimizing coil configurations to enhance energy transfer efficiency in DWPT systems, introducing a novel Vertical Coil (VC) configuration and comparing its performance to the established Double-D Quadrature (DDQ) system.

Inductive power transfer (IPT), the core mechanism of DWPT, relies on alternating magnetic fields generated by transmitter coils inducing currents in receiver coils. However, IPT's efficiency decreases significantly over mid-range distances, such as the 30 cm air gap between road and vehicle chassis. Magnetic Resonance Coupling (MRC) addresses this challenge by synchronizing transmitter and receiver coils at resonant frequencies, enhancing energy transfer efficiency and system impedance matching.

This thesis presents a systematic analysis of DWPT configurations through simulations and experimental models. The study emphasizes optimizing coil geometry, spacing, and mutual inductance to achieve higher energy transfer rates. The VC configuration employs vertical rectangular coils encasing a ferromagnetic core to enhance magnetic field alignment, while the DDQ system utilizes horizontal coils with a ferrite plate for magnetic guidance. Comparative analysis of full-scale and small-scale models revealed significant performance disparities.

The VC system demonstrated a maximum efficiency of 93%, surpassing the 85% peak efficiency of the DDQ configuration. Moreover, over a single pass, the VC system transferred more than 50% additional energy compared to the DDQ system, highlighting its superior capacity for efficient energy transfer in dynamic conditions. Furthermore, the VC system maintained efficient energy transfer over broader ranges, facilitated by improved magnetic field alignment and mutual inductance optimization. Experimental validation confirmed the reliability of simulation results, showcasing the VC system's potential to outperform existing technologies in real-world applications. However, challenges remain, including managing resonance frequency shifts and maintaining consistent coupling under dynamic conditions.

Future research directions include exploring coil dimensions, increasing receiver coil numbers, and integrating superconducting materials to enhance system efficiency. As a culmination of this work, we are currently at the publication stage of a scientific article, and a patent based on these findings has been submitted. This study contributes significantly to

advancing DWPT technologies, supporting the global transition to sustainable transportation solutions by providing a scalable and efficient wireless charging alternative.

Introduction

The global transition towards sustainable energy solutions has driven significant advancements in the field of electric vehicles (EVs). One of the critical challenges to widespread EV adoption is achieving efficient and practical energy charging infrastructure. Traditional charging methods require long time charging at specific points, limiting the range and operational efficiency of EVs. As a response to this challenge, Dynamic Wireless Power Transfer (DWPT) has emerged as a promising solution, enabling vehicles to charge while in motion without the need for stationary charging stops [2-4].

DWPT systems transfer energy between transmitter coils embedded in the road and receiver coils attached to the vehicle. This continuous charging process reduces the need for large battery storage on vehicles, leading to lighter EVs, improved energy efficiency, and significant environmental benefits through reduced CO_2 emissions [7] and hazardous waste from battery production [8-11]. This technology leverages inductive coupling, a wireless power transfer (WPT) method that facilitates energy transfer without direct contact between the transmitter and receiver.

The fundamental principle of inductive power transfer (IPT) lies in Faraday's law of induction, where an alternating current passing through a coil generates an alternating magnetic field, which induces a current in a nearby coil. However, inductive coupling is highly sensitive to the distance between the primary and secondary coils, making it challenging to apply in dynamic scenarios with larger air gaps, such as the gap between the road and the vehicle chassis. Magnetic Resonance Coupling (MRC) [12] has been proposed to address this challenge by enhancing energy transfer efficiency over mid-range distances. MRC leverages the resonance phenomenon, where both the transmitter and receiver coils operate at the same resonant frequency, maximizing energy transfer and improving the overall efficiency of the system. The resonance frequency is identified as the point at which the system achieves maximum power transfer, indicated by the peak in the measured spectrum. This is because, at the resonance frequency, the system's impedance is optimized, maximal current is flowing through the transmitter and receiver circuits allowing for a maximal energy transfer.

In this work we describe a novel configuration of DWPT coils layout suggested by our research group at the department of Physics, Bar-Ilan University. We focused on optimizing the design of receiving coils to improve energy transfer efficiency in DWPT systems for electric vehicles. we explore a new vertical coil configuration for the receiver and evaluate the performance through simulations and experimental models. The primary goal of this research is to assess the efficiency of this innovative coil configuration and compare it with existing state of the art system.

This research integrates both simulation-based analyses and experimental validation to evaluate the performance of small-scale models representing the configuration commonly used in commercial applications and the newly proposed Vertical Coil (VC) configurations. By systematically measuring the operational efficiency of these models and comparing the experimental results to simulation predictions, the study aims to assess the practicality and viability of these coil designs for real-world Dynamic Wireless Power Transfer (DWPT) applications.

The outcomes of this research will contribute to the ongoing development of more efficient and sustainable wireless charging technologies for electric vehicles, supporting the global shift towards greener transportation solutions.

Inductive Power Transfer

The term "inductive power transfer" (IPT) [6] refers to the process of transferring energy between inductors without any physical contact, thus enabling wireless power transfer (WPT). Currently, IPT is the predominant method for short-range WPT applications, with the transformer being the most common example.

When an alternating current (AC) flows through a transmitter coil, it produces an oscillating magnetic field. This oscillating field partially penetrates a receiving coil, inducing an alternating voltage within it in accordance with Faraday's law of induction. Faraday's law is expressed as:

$$1.\quad \epsilon = -\frac{\partial \phi_B}{\partial t}$$

where ϵ is the induced electromotive force (emf), and $\frac{d\phi_B}{dt}$ is the magnetic flux through the coil.

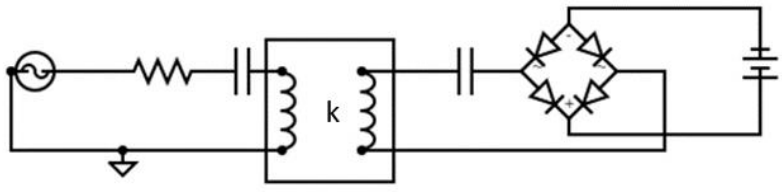

Figure1- Inductive Power Transfer. The transmitter coil from the left is generating magnetic flux and Some of the magnetic flux is picked up by the receiver coil (from the right), which is connected to a battery.

Figure 1 schematically illustrates a typical 2-coil scenario [13]. The transmitting coil powered by an oscillating voltage source. The receiving coil, is positioned at a certain distance from The transmitting coil and is connected to the load through a rectifying circuit element. "K" indicates the coupling coefficient , namely, the part of the flux lines that are generated in the

transmitter cross through the receiver coil. Since some field lines close in space without interacting with the receiving coil, the coupling between the coils is always smaller than 100% and falls dramatically as the gap between the coils increases. The degree of magnetic flux coupling between the coils is quantified by the mutual inductance (M) of the transmitter and receiver coils, defined as:

$$2.\quad M_{12} = \frac{V_2}{\left(\frac{dI_1}{dt}\right)}$$

where I_1 denotes the current flowing through the transmitter coil, and V_2 signifies the induced voltage across the receiver coil. The mutual inductance between the coils allows us to define the electromagnetic coupling coefficient, K , between the transmitter and receiver. This coefficient, K, represents the proportion of magnetic flux generated by the transmitter that is captured by the receiver.

$$3.\quad k = \frac{M_{12}}{\sqrt{L_1 * L_2}}$$

Where L_1, L_2 are the self induction of the transmitting and receiving side respectively and M is the mutual inductance.

Classic inductive coupling is highly effective for near-field applications, where energy transfer relies on the close proximity of the transmitting and receiving coils. In these cases, the coupling coefficient K a measure of the fraction of magnetic flux from the transmitter that links to the receiver is typically close to 1 (100%). This ensures efficient energy transfer and makes the method suitable for applications like transformers and small appliance chargers. However, as the distance between the coils increases, the coupling coefficient decreases significantly, leading to a drop in the amount of energy transferred.

For mid-range applications [14], such as wireless charging for electric vehicles (EVs), the air gap between the road and the vehicle chassis approximately 30 cm reduces K to around 10% or less. This low coupling poses a substantial challenge, as it reduces the mutual inductance between the coils, which is essential for efficient power transfer. However, it's important to note that a low coupling coefficient does not equate to energy loss. Energy that is not transferred to the receiver is not dissipated. instead, it remains in the system and is effectively returned to the source. This opens opportunities to enhance system design without significant energy wastage.

To address the limitations of low coupling in EV charging, magnetic resonance coupling is employed. Unlike standard inductive coupling, this method utilizes resonant circuits on both the transmitting and receiving sides, which are tuned to the same frequency. By operating at resonance, the system maximizes energy transfer efficiency even over larger air gaps. This allows for practical and effective mid-range wireless power transfer, overcoming the limitations of conventional inductive methods.

Resonance

To overcome the challenges of low coupling coefficient K in mid-range wireless power transfer, Magnetic Resonance Coupling (MRC) [15] offers a highly effective solution, particularly for applications like electric vehicle (EV) charging. MRC relies on the principles of resonance to significantly enhance energy transfer efficiency over larger distances. An intuitive way to grasp this concept is to compare it to the motion of a swing. When you push a swing at random intervals, the energy imparted is inefficient and uncoordinated, resulting in minimal motion. However, if you push the swing at its natural frequency—its resonance point—each push builds upon the previous one, rapidly increasing the swing's amplitude with relatively small, consistent inputs of energy. This resonance effect amplifies the energy transfer significantly.

In the context of MRC, energy is not transmitted in a single, large burst but rather in small, synchronized "packets" at the resonant frequency of the system. Both the transmitter and receiver coils are part of electric circuits tuned to the same frequency. When these circuits resonate, energy oscillates between the transmitter and receiver efficiently, minimizing losses and enabling the transfer of much higher amounts of energy wirelessly, even over larger air gaps. This resonance-driven approach is what makes MRC a transformative method for mid-range applications like dynamic EV charging.

In the implementation of resonance coupling for wireless power transfer, energy is still transferred inductively. However, both the transmitter and receiver coils are connected to their respective resonator circuits. When these resonators are tuned to the same resonant frequency, power can be transferred much more efficiently and across larger air gaps. The impedance of a simple RLC series circuit (as shown in Fig. 1) can be expressed by the following formula:

$$4.\quad Z = R + i(X_L + X_C)$$

$$5.\quad X_L = \omega L\ , X_C = -\frac{1}{\omega C}$$

It is evident that when $X_L = X_C$,minimal impedance is achieved, resulting in minimal alternating current (AC) resistance. At this resonant frequency, reactive energy oscillates between the coil and the capacitor, accumulating with each cycle of the source. Because some energy is inevitably lost due to circuit resistance, the quality factor, (Q), of both the

transmitter and receiver circuits must also be considered. The quality factor is defined as the ratio of the energy stored in the circuit to the energy dissipated by the impedance of the circuit. For the series resonator discussed above, (Q) is given by:

$$6.\quad Q = \frac{\omega_0 L}{R} = \frac{1}{R\omega_0 C}$$

Where ω_0 is the self frequency of the system. Using these parameters, the impedance of a series resonator can be represented as follows:

$$7.\quad Z = \sqrt{\frac{L}{C}} \cdot \left[i\left(\frac{\omega}{\omega_0} - \frac{\omega_0}{\omega}\right) + \frac{1}{Q} \right]$$

In Wireless Power Transfer (WPT) systems, the quality factor (Q)-a measure of how effectively energy oscillates within the system-is typically in the range of a few hundred. This high Q value indicates that the system can store and transfer energy efficiently between the transmitter and receiver when operating at resonance. A higher Q factor reduces energy losses during oscillations, directly contributing to improved system efficiency, especially when the system is finely tuned to the resonance frequency. This ensures maximum power transfer with minimal dissipation.

When the system is tuned to its resonant frequency, the alternating current in the transmitter creates an oscillating magnetic field that efficiently couples with the receiver. At resonance, the energy builds up within the system due to constructive interference between oscillations, leading to a significantly higher induced voltage in the receiver coil. In fact, this voltage can be orders of magnitude higher than what is achievable in a non-resonant inductive power transfer (IPT) system.

This phenomenon can be measured and observed in the voltage across the receiving coil or the load connected to it. For instance, when the system operates at resonance, the output voltage spikes dramatically, which can be visualized using an oscilloscope or analysed via a vector network analyser (VNA) by observing a sharp dip in the impedance at the resonant frequency. In our case, we had to short the circuit during the VNA measurements because the input power was insufficient to activate the diode bridge, as shown in Figure 1. This adjustment impacted the results of the VNA measurements, as will be shown later.

The energy calculations make sense when considering the resonance behavior of an RLC circuit. Reactance refers to the opposition that inductors and capacitors provide to alternating current, with inductive reactance increasing with frequency and capacitive reactance decreasing with frequency. At resonance, the reactance of the inductor and capacitor cancel each other out, minimizing the circuit's overall impedance. This cancellation allows for maximal current flow and, consequently, maximal power transfer. Additionally, the energy

stored in the oscillating magnetic field is repeatedly transferred back and forth between the transmitter and receiver with minimal losses, thanks to the high Q, leading to the observed increase in induced voltage. Without resonance, this energy transfer efficiency is significantly diminished, resulting in a much lower induced voltage.

$$8.\quad P = \frac{1}{T}\int_0^T I(t) \cdot V(t)dt$$

$$9.\quad \eta = \frac{P_{receiving}}{P_{transmitting}}$$

To measure the efficiency, we calculated the power on both the transmitting and receiving sides of the system. On the transmitting side, the average power was determined using Equation 8, which incorporates the time-dependent voltage and current of the source or the receiving end. we define the system's efficiency, is defined as the ratio of the power at the source divided by the power at the load.

DWPT-Dynamic Wireless Power Transfer

In the realm of transportation, achieving a state where vehicles do not need to stop for fuelling or charging represents an ultimate goal. This would enable unlimited travel time and unlimited range, which translates to continuous service of EVs in public transportation. Although this idea may seem fictional, one emerging technology shows promise in realizing this vision: Dynamic Wireless Power Transfer (DWPT) [1]. Over the past decade, DWPT has been gaining popularity. By applying energy transfer methods to moving systems, it is theoretically possible to achieve dynamic charging for electric vehicles (EVs), thus supporting the desired unlimited travel range and time. As we'll describe below, ongoing worldwide projects demonstrate that this target is feasible and achievable.

Designing an effective Dynamic Wireless Power Transfer (DWPT) configuration requires addressing numerous variables and challenges, particularly during even the simplest driving segments.

- critical factor is the mutual inductance, which is determined by the relative positions of the coils. The transmitter coils are fixed in position, embedded beneath the road while the receiver coils are attached to the EV's chassis and travel with it as the coils move, their changing locations directly impact the mutual inductance, which in turn affects the coupling between the transmitting and receiving coils, as well as the coupling among the receiving coils themselves.

- Another significant challenge is maintaining resonance frequency during motion. As previously mentioned, the mutual inductance changes as the coils move. This variation in mutual inductance directly affects the resonance frequency of the entire system. When the resonance frequency shifts, the system can no longer operate within a specific narrow band of frequencies, leading to reduced efficiency and difficulty in achieving optimal energy transfer. Managing these fluctuations is crucial for ensuring consistent performance in dynamic conditions.
- Practical the size of the coils determines the shape and extent of the magnetic field generated. If the model's dimensions are not optimized, the magnetic field may not align effectively with the receiving coils. This misalignment can lead to poor coupling and reduced energy transfer efficiency. For example, overly large coils may produce areas of magnetic flux that cancel out due to opposing field lines, while undersized coils might not generate a strong enough field to cover the receiving area.
  The presence of metallic parts near the system can also lead to losses by generating eddy currents within the metal. These currents divert energy that would otherwise be transferred to the receiving coils, reducing the system′s overall efficiency.
- The nonlinearity of ferrite materials adds significant complexity. As will be described later, Ferrite plates are used in the vicinity of the receiving and⁄or transmitting coils to concentrate, divert and screen magnetic field. Their strong non-linear dependence of the magnetization on the external magnetic field, strongly affect the self- and mutual inductance of the coils nearby. Therefore, the coupling coefficient becomes dependent of the momentary current flowing in the transmitting coils and its dependence of the relative distance between the transmitting and receiving coils strengthens even further. Moreover, when the Ferrite reaches It no longer serves its purpose. More precisely, the entire magnetic field distribution in the space surrounding the coils varies with the internal magnetization state of the ferrite. The ferrite also exhibits magnetic hysteresis namely, a lag between the applied magnetic field and the resulting magnetization, which results in energy losses during each cycle of the alternating current (AC). In high-frequency applications, such as WPT systems, these losses become significant , degrade the Q factor, and can lead to localized overheating. Prolonged exposure to such conditions can compromise the structural integrity of the ferrite, causing microcracks or fractures that further degrade its performance. Thus , careful design and operating limits must account for the ferrite′s nonlinearity, ensuring that the system remains within safe magnetic field and temperature thresholds [16].
- Frequency splitting [17] is a phenomenon observed in resonant Wireless Power Transfer (WPT) systems when the coupling coefficient K between the transmitting and receiving coils is high enough. In such cases, instead of having a single resonant frequency where maximum power transfer occurs, the system exhibits two distinct

resonance peaks, splitting the frequency spectrum. This effect is a result of the strong coupling between the coils, which introduces an additional degree of interaction between the resonators, effectively creating two modes: an in-phase (low-frequency) mode and an out-of-phase (high-frequency) mode.

Mathematically, this can be understood by examining the total impedance of a resonant system consisting of two coupled resonators. The system's resonance conditions are derived from the mutual inductance M,inductances(L_1, L_2) ,and the associated capacitances (C_1, C_2). The resonance frequencies are given approximately by:

$$f_{res,split} = \frac{1}{2\pi}\sqrt{\frac{1}{LC} \pm \frac{M}{L^2}} \quad (10)$$

where M is the mutual inductance, L and C are the self-inductance and capacitance of the coils, respectively, and the $\pm\frac{M}{L^2}$ term introduces the splitting.

Frequency splitting has direct implications for impedance matching, which is crucial for maximizing power transfer. In a WPT system, the maximum power transfer occurs when the impedance of the source matches the impedance of the load, as described by the maximum power transfer theorem. However, at high coupling levels, the introduction of the two resonance peaks can complicate this matching. If the operating frequency is not tuned precisely to one of the split resonance frequencies, the system's impedance will deviate from its optimal value, reducing power transfer efficiency. Impedance matching in this context often involves tuning the source or load to align with one of the split resonance frequencies. This is achieved by adjusting the capacitors in the circuit to counteract the effects of the mutual inductance and maintain the system's resonant condition at the desired operating frequency. To maintain efficient power transfer in the presence of frequency splitting, careful consideration must be given to the coupling coefficient and the system's operating frequency. If K is too high, the split frequencies can drift far apart, making it challenging to design the system for a narrow-band operating frequency.

These dynamic variations must be carefully managed to ensure consistent and efficient energy transfer. This research addresses several of these issues, including variations in the coupling coefficient during motion, and position-dependent resonance frequency, all of which impact the energy transfer efficiency of DWPT systems. Over the years, various configurations have been tested to address these challenges. Here we focus on two of the most significant realization concepts worldwide: the state-of-the-art DDQ[5] configuration and our proposed innovative configuration, termed Vertical Coils (VC).

The DDQ configuration (to be described in the following section) has demonstrated significant progress in the field of DWPT. This system is expanding globally, with multiple worldwide pilot and commercial projects Electreon Ltd., an Israeli company, is one of the world's leading innovators in the field of Dynamic Wireless Power Transfer (DWPT). The company has deployed its technology in numerous countries, including Italy, Germany, Sweden, Michigan (USA), Norway, France, China, and Israel.

Despite these advances, significant work remains to optimize this technology and enhance its energy efficiency. The following section will explore the new configuration we propose, examining how changes in the system's topology contribute to progress in energy efficiency.

DWPT State-of-the-art

The development of Dynamic Wireless Power Transfer (DWPT) systems has been an area of extensive research and innovation, driven by the need for efficient and continuous charging solutions for electric vehicles (EVs). Over the years, various configurations and methodologies have been explored to overcome the unique challenges posed by DWPT, such as maintaining effective energy transfer over varying distances, addressing misalignments, and ensuring system stability during motion. This section reviews the significant advancements in DWPT technology, highlighting key contributions from academic and industrial research. These works provide the foundation for understanding the current state-of-the-art and the ongoing efforts to optimize DWPT systems for real-world applications.

1. In 2010,a group from the Korea Advanced Institute of Science and Technology (KAIST) suggested a new configuration that the "I-type" configuration that shown in Figure 2 . In this configuration, the ferrite is shaped like the letter "I" and the cables carrying the current are placed on both sides of the ferrite, intensifying the field in the core This solution provides effective spatial magnetic coverage on the road for short distances between the pickup layout and the "I" core. However, its performance declines as the distance increases because the magnetic flux lines on the transmitting side tend to close between the upper and lower parts of the "I" shape. This behavior limits the magnetic field's reach and significantly reduces coupling efficiency at greater separations. [18-20].

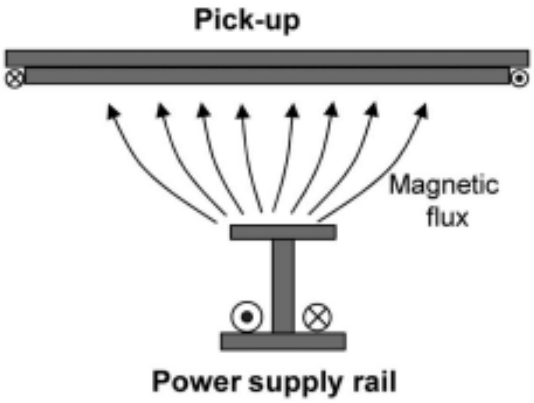

Figure 2–"I" shape configuration to DWPT system

2. In 2014, the Korea Advanced Institute of Science and Technology (KAIST) showed that it is possible to achieve an efficiency of about 80% at high power levels in energy transfer at a distance of 26 cm from the transmitting coil to the receiver. The system described consists of a transmitting cable that arrives from one side and bends 180 degrees towards the direction it came from in order to increase the amount of field collected from the receiving coils, as seen in Figures 3.a+3.b. In addition, there are ferrite plates whose role is to "navigate" the magnetic field in an optimal way to the receiving coils. The receiving coils are shown at the top of the figure 3.a. There are three coils with ferrite cores attached to each of the coils. The simulation we made and is presented in Figure 3.c illustrates the magnetic field distribution and the direction of the propagating flux for the transmitter and the ferrite. This visualization highlights how the magnetic field is shaped and guided by the ferrite material, providing insights into the interaction between the transmitter and its surroundings. The reason for the three coils is the shape of the magnetic field. If there was one coil, the total flux would be 0, and with 3, the magnetic flux that returns back to the system is also collected [21].

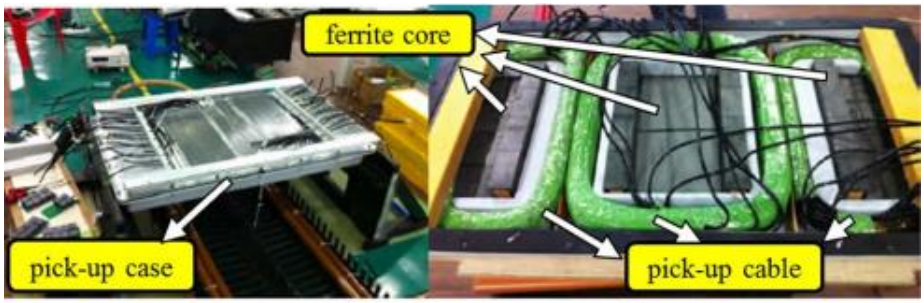

Figure 3.a -receiving side of the DWPT

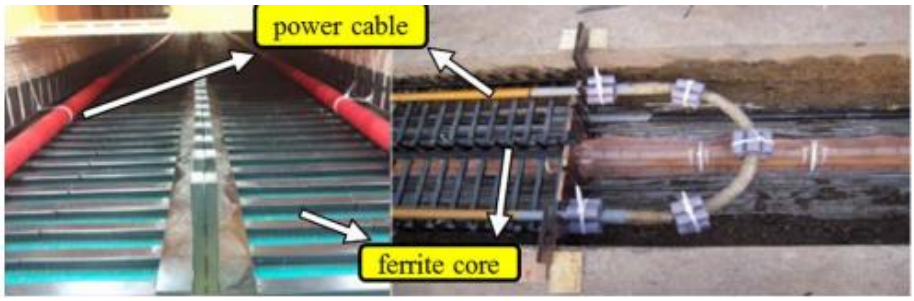

Figure 3.b -transmitting side of the DWPT

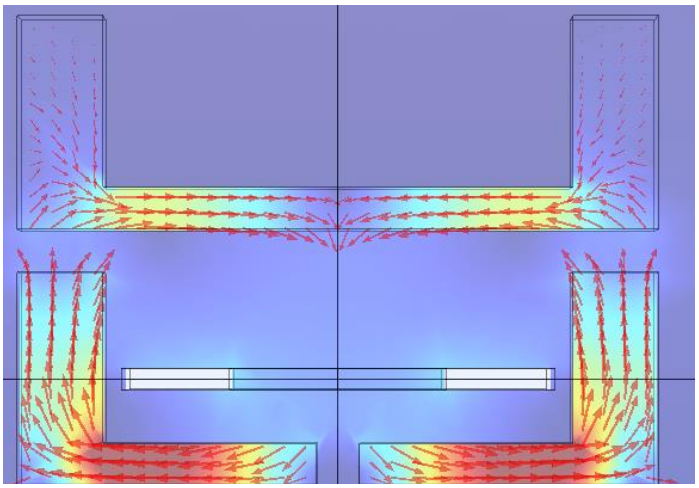

Figure 3.c -picture of the magnetic field distribution and direction at log scale at COMSOL

3. Another variation is the "S-type" configuration shown in Figure 4. This configuration provides a slightly different distribution of the transmitting coils. It is also named for the shape of the ferrite, which resides in the transmitting area and in the upper and lower areas of the "S". Opposing current carrying cables are placed inside the ferrite structure in a manner similar to the "I" shape design [22-23].

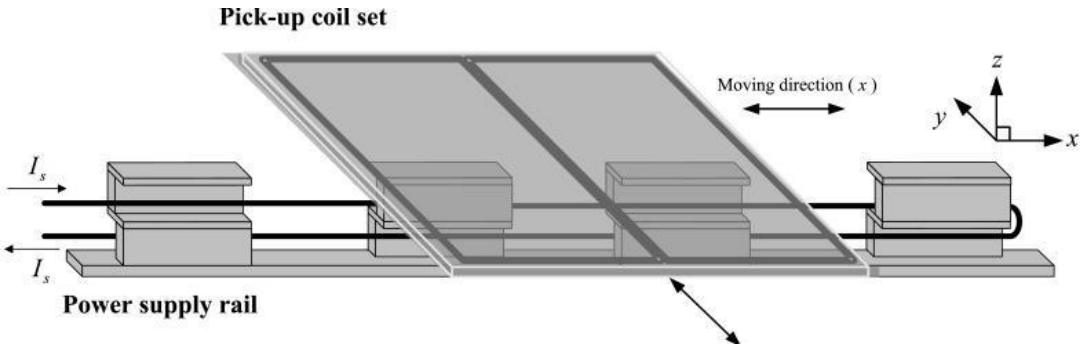

Figure 4–"s" shape configuration to DWPT system

In both the "I-type" and "S-type" configurations, it was understood that while the distribution of the magnetic field in space provides a certain advantage, a significant disadvantage is found in the low coupling between the transmitting and receiving coils.

4. Research conducted by a group at the University of Hanoi in Vietnam in 2021 demonstrated that at very short transmitter-receiver gaps (around one centimetres), a transfer efficiency of approximately 94% could be achieved. However, as thise distance increases to around six centimetres, the transfer efficiency drops to 78%. The system consists of three horizontal transmitting coils placed close together, as shown in Figure 5. The outer coils carry current in a counterclockwise direction, while the middle coil carries current clockwise, effectively increasing the number of flux lines that reach the receiving coil. The transmitting coils are connected in a bipolar arrangement, resulting in a circular magnetic field between each pair of transmitting coils.
   Beneath the transmitting coils is a layer of ferrite material that collects and transmits the magnetic flux, enhancing the efficiency of power transfer. Above the receiving coil, there is an aluminium plate that serves as a shield against external magnetic interference by generating eddy currents. These eddy currents help reduce stray magnetic fields, thereby protecting the driver and passengers from exposure to high levels of non-ionizing radiation [24].

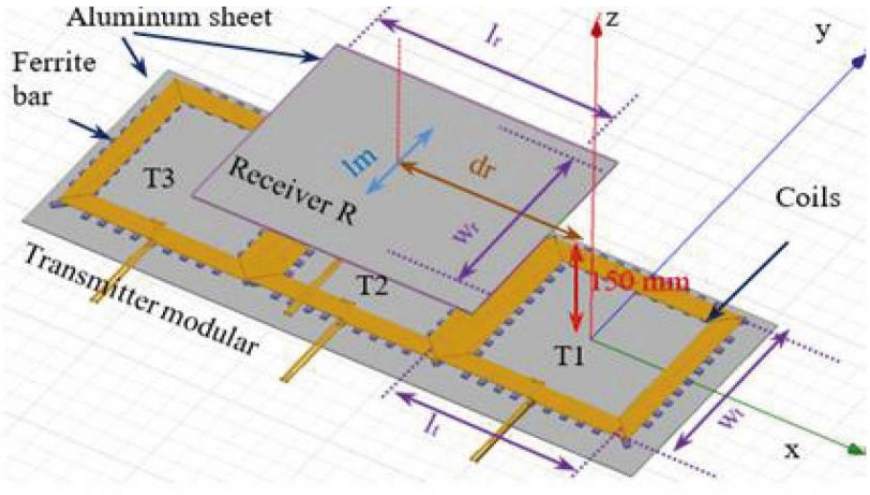

Figure 5–configuration that invented at Vietnam at 2021

5. In 2021, Sahar Barali examined the configuration of two transmitting coils and receiving coils in a DDQ structure with a ferrite plate mounted above in his master's thesis at the Bar-Ilan Institute for Superconductivity as we can see at figure 6. Barali examined the effect of the dimensions of the coils on the efficiency and showed that for each size of transmitting coil there is an optimal size of receiving coil. The energy efficiency increases as the coil is increased up to this point, from where it starts to decrease with the increase of the coil. The phenomenon was explained by analysing the spatial distribution of the magnetic field, which showed that in coils that are too large, positive and negative fluxes that reach the coil cancel each other out. Barali also showed that it is possible to achieve a system efficiency of over 80% at a distance of about 30 cm between the transmitting and receiving coils. Today, this configuration is used by commercial companies such as Electreon, but as mentioned, there are great efforts being made worldwide to find a more efficient configuration.

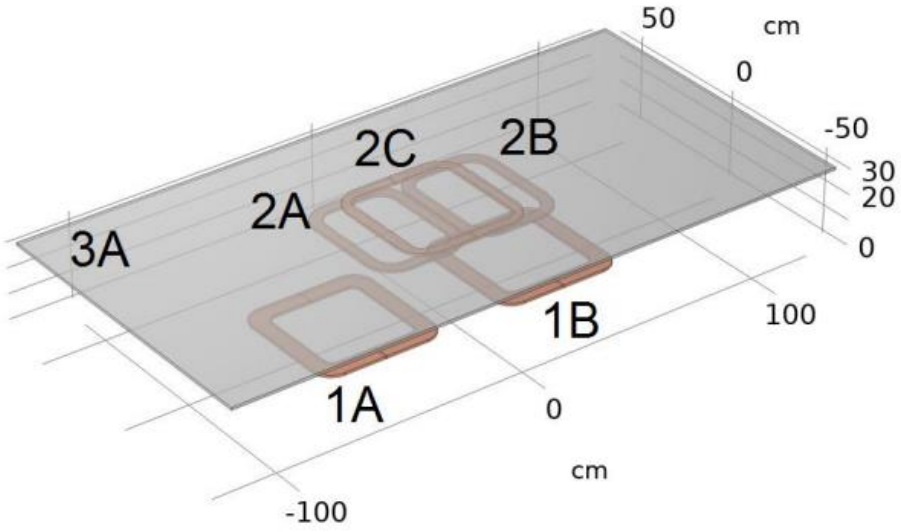

Figure 6– DDQ configuration at Bareli's system

All these configurations aim to optimize a single critical aspect: the spatial magnetic field. This is achieved by altering the geometry of the coils or incorporating ferromagnetic materials to shape and direct the magnetic flux more effectively. These modifications are designed to enhance coupling efficiency and maximize energy transfer to the receiving coils [25].

State of the art

As previously mentioned, the DDQ configuration has been widely considered the optimal approach for wireless power transfer. However, recent research is exploring alternatives. Let's dive into some of the newest studies published in this area.

1. In 2023, the Faculty of Electrical Engineering and Computer Science at the University of Maribor, Slovenia, published an article describing a new configuration using DDQ coils as shown in figure 7. They employed DDQ coils for both the transmitting and receiving ends. For the transmitting coils, they took DD coils and stacked another set of DD coils on top, rotated 90 degrees on the XY plane. They named this configuration 2DD. Finally, they added a Q coil above the 2DD. The complete set of transmitting or receiving coils was thus called 2DDQ.The receiving coils followed the same principle. A ferrite plate was placed blow the receiving coil and above the transmitting coils to guide the magnetic field.

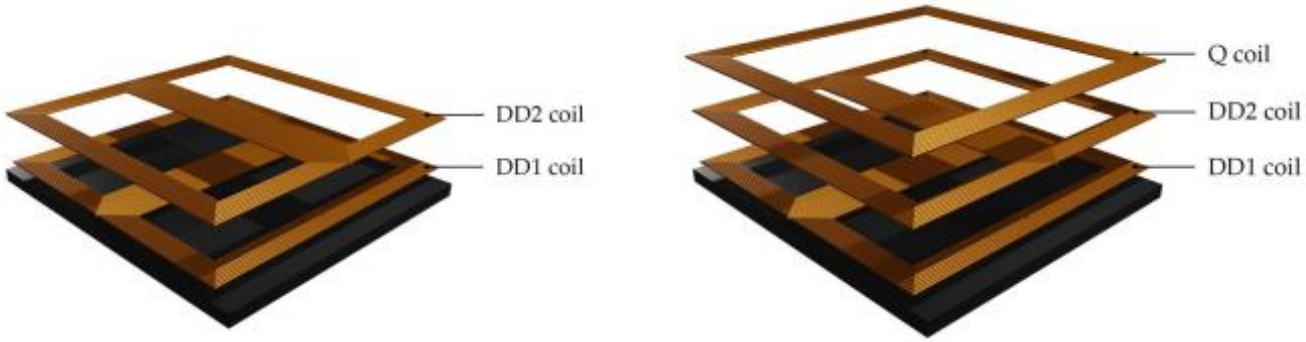

Figure 7– mixed axis of DDQ system

The advantage of this method is that there is no magnetic coupling between individual receiving and transmitting coils. This means the magnetic field is not affected by nearby coils and couples only with the corresponding coil on the other side. In this article, the authors measured the efficiency of a 2DD-2DD system and a 2DDQ-2DDQ system at various distances between the transmitting and receiving sides. They also investigated the effects of movement along the X and Y axes. All the results showed a maximum energy transfer efficiency of around 75% to 78% [26].

2. In 2023, Chongqing University, Chongqing, China. Published an article about DWPT system with DD coils at the transmitting side and at the receiving side. In this article they plaed a ferrite plate above the receiving coils. Each DD coil at the transmitting side is connected to its own inverter as we can see in figure 8. The innovation of this work is that they execute this system to their public transportation. Also, they added to the system a feature that activates the transmitting coils only when the bus is passing above, (RX and TX in fig. 8 are the receiving and transmitting coil respectively [27].

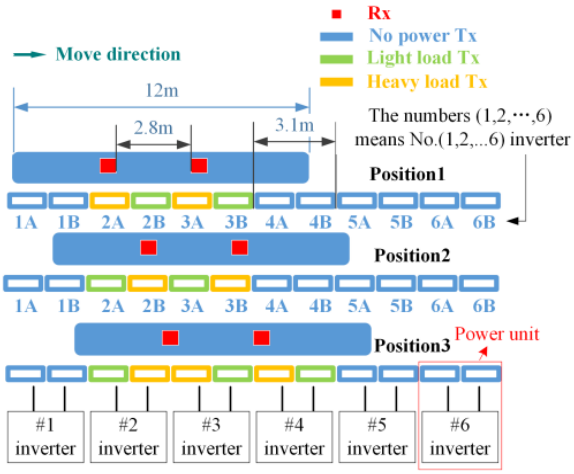

Figure 8– 60 KW WPT system of DD at the transmitting and the receiving

Transmitter Configuration

The typical way to build a Wireless Power Transfer (WPT) system includes an AC voltage source, a transmitting circuit, a receiving circuit, a rectifier, and a load that can be either a resistor or a battery, as depicted in Figure 1. Both the DDQ and VC systems share the same transmitting configuration to facilitate a comparison of the receiving side. The transmitting setup consists of two bipolar cubic horizontal coils made from litz wire, each with 11 turns, inner length of 4.8cm, out length of 5cm and 0.4cm height as shown in Figure 9.

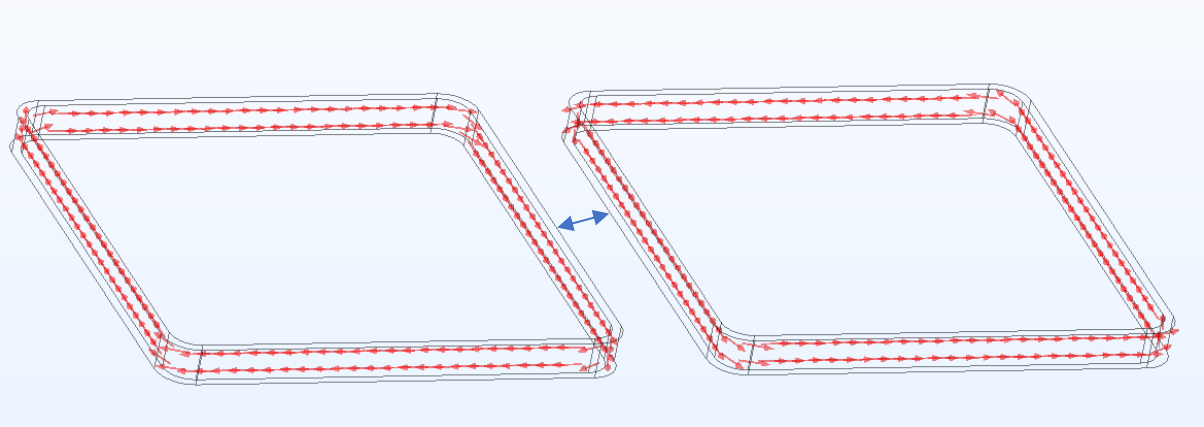

Figure 9- current arrow direction at transmitting two bipolar coils ,the blue double sided arrow is the gap between the coils .

This configuration creates a circular magnetic field between the two coils and two elliptical magnetic fields on the right and left sides of the coils. Figure 10 illustrates the logarithmic magnetic field distribution, showcasing these distinct field patterns.

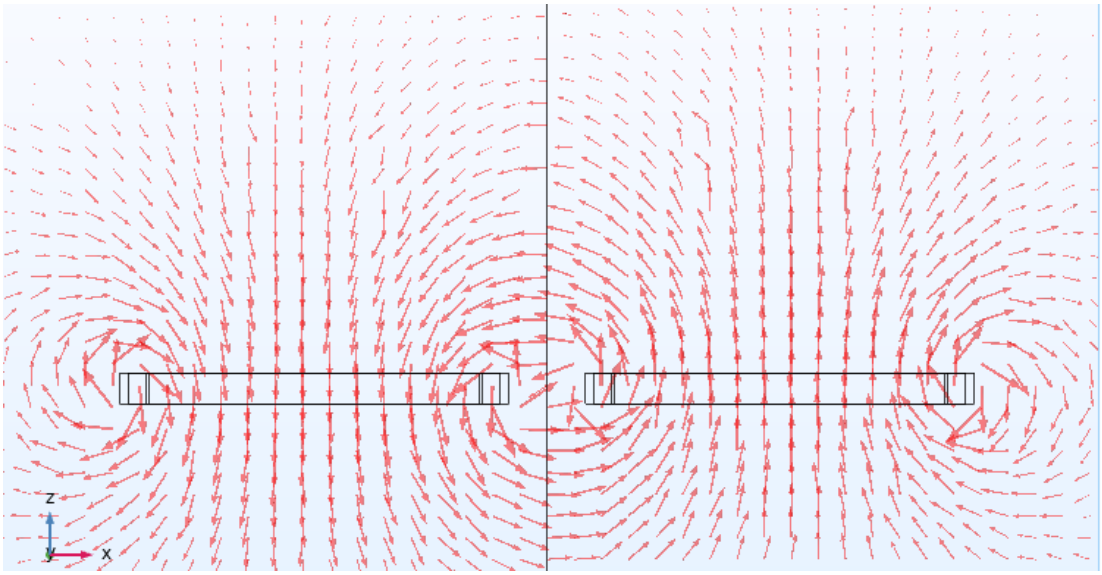

Figure 10- side look of the magnetic field at log scale from the transmitting coils

Next, we add a ferromagnetic material, ferrite. The ferrite is the best fit for use in DWPT applications because of its relatively low loss high-performance capabilities in high operation frequencies. This material reshapes the magnetic field distribution in space due to several reasons:

1. Ferrite is an ideal material for magnetic field management due to its exceptional magnetic properties. Its high magnetic permeability allows it to become easily magnetized, providing a low-resistance path for magnetic field lines. This makes ferrite highly effective as a concentrator and diverter of magnetic flux. Additionally, the alignment of microscopic magnetic domains within ferrite under an external magnetic field reduces the system's overall energy, enhancing its ability to efficiently channel the magnetic field. Ferrite's low magnetic reluctance, analogous to low electrical resistance in a circuit, minimizes opposition to magnetic flux, enabling more field lines to pass through. As a result, ferrite concentrates magnetic field lines within itself, creating a stronger and more focused magnetic field compared to non-magnetic materials.
2. Ferrite exhibits hysteresis, where the material's magnetization depends on its magnetic history. Once magnetized, ferrite can retain a significant amount of magnetization, further enhancing its ability to channel magnetic fields. However, ferrite can also reach saturation, where increasing the external magnetic field no longer significantly increases magnetization.

In summary, ferrite is preferred for shaping magnetic fields because it can easily become magnetized and conduct magnetic lines of force with minimal opposition, making it highly efficient in concentrating and channeling magnetic flux. This effect can be observed in Figure 11, which shows the magnetic field with ferrite, where the upper rectangle represents the ferrite material.

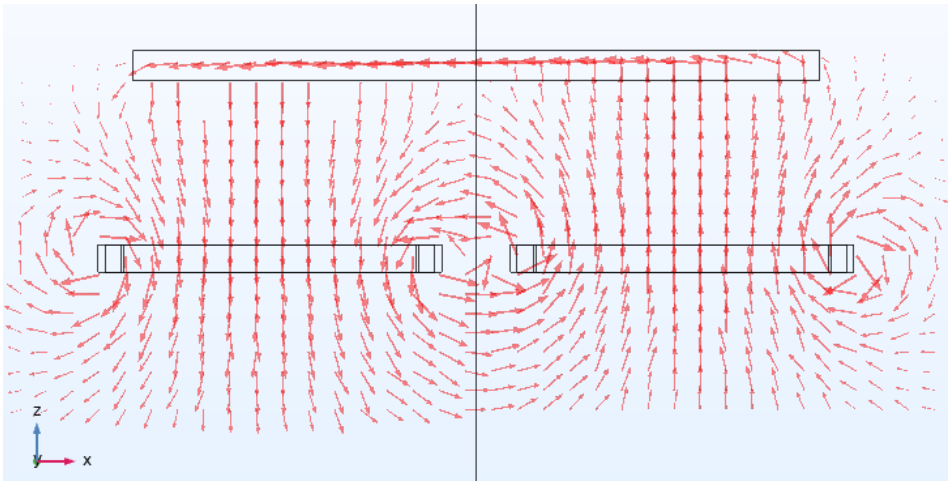

Figure 11-magnetic field generated from the transmitting coils with ferrite at log scale

Receiver Configuration

The main focus in this work is the receiver. The DDQ is the state-of-the-art configuration in use in pilot and commercial projects worldwide while the VC is our innovative configuration. We will now discuss the differences between these configurations.

The DDQ receiver consists of two bipolar coils, referred to as "DD," with an additional coil, called "Q," positioned centrally above them. A ferrite plate in mounted on top of the DDQ layout. Each of the DD and Q coils is connected to a separate RLC circuit to achieve the resonance state.

Similar to the transmitter coils, the DDQ coils are also horizontal mounted and are made from litz wire.

In figure 12.a, we can observe the smaller model of the DDQ system. This model helps in verifying the simulation accuracy by comparing the measured performance of the physical model with the simulation results.

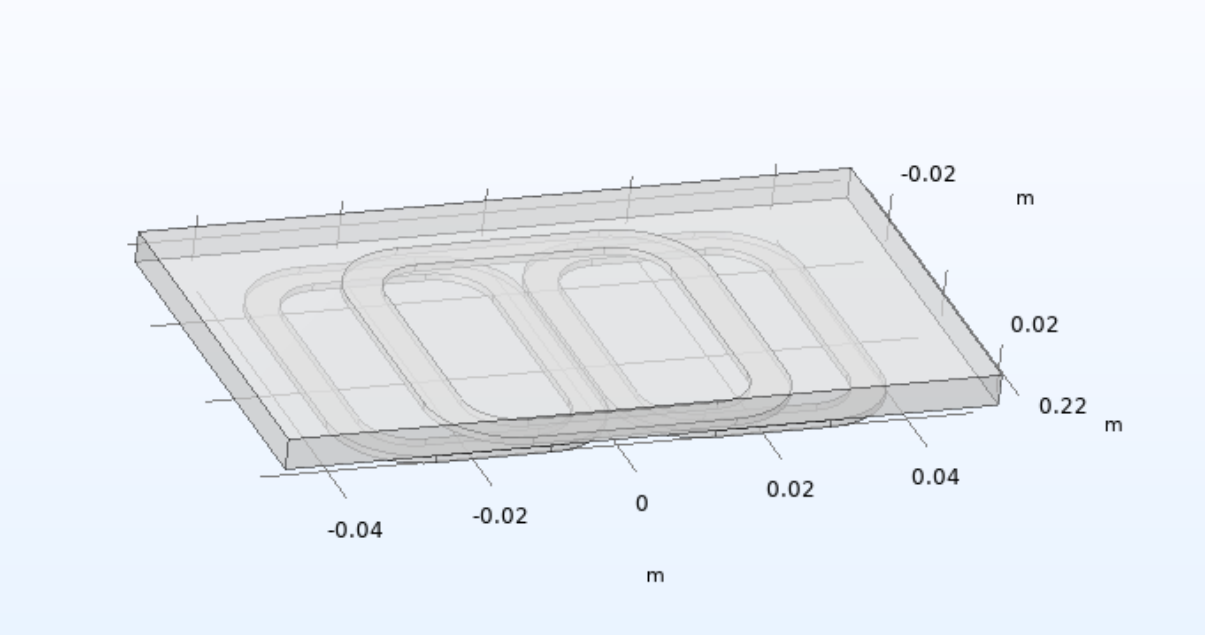

Figure 12.a-small DDQ receiver configuration

The graph at figure 12.b shows the coupling coefficient k as a function of position (x) for the DDQ configuration, with individual contributions from the D1, D2, and Q coils clearly

separated. One of the key strengths of the DDQ configuration is evident in this graph: at every point during movement, at least one coil contributes significantly to the coupling, ensuring continuous energy transfer.

As the vehicle moves along the xx-axis, the coupling of D1 and D2 rises and falls alternately, while the QQ coil provides additional coupling in areas where D1 and D2 contribute less. This staggered behaviour creates a seamless overlap, minimizing gaps in energy transfer. The dynamic interplay among the three coils ensures efficient coupling across the entire motion range, making the DDQ configuration particularly effective for dynamic wireless power transfer systems.

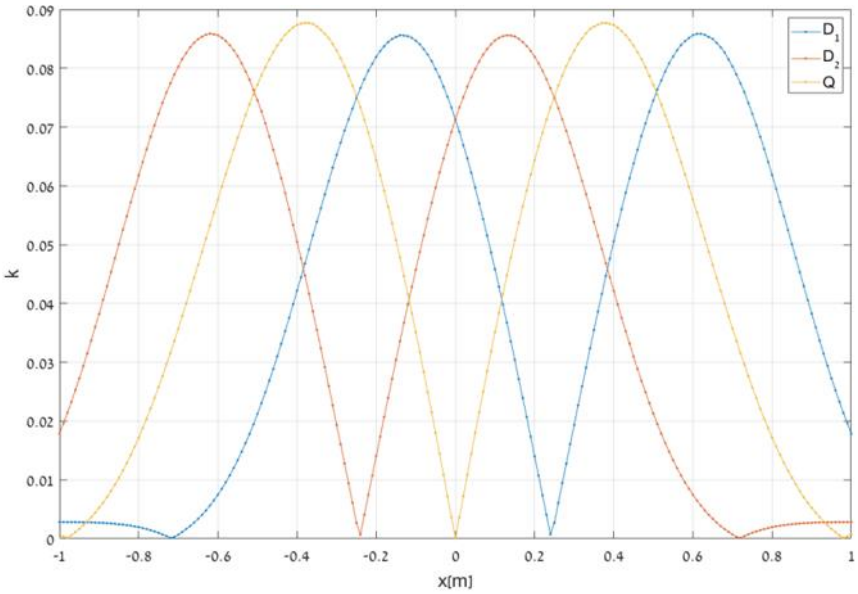

Figure 12.b-the coupling while movement of the DDQ configuration

After introducing the DDQ configuration, we sought ways to improve it to achieve higher energy transfer efficiency. This led to the development of the novel Vertical Coil (VC) configuration, designed to address this challenge. Historically, this approach was not explored because it was assumed that the limited space between the bottom of the car and the road (approximately 30 cm) would be insufficient to accommodate such a design. However, we proposed a solution with smaller, vertically oriented coils that fit within the available space while significantly enhancing energy transfer performance.

This method is expected to outperform the DDQ configuration because it takes advantage of the denser magnetic flux lines that are horizontal within the ferrite compared to the weaker vertical flux lines outside the ferrite. Additionally, we observed that the magnetic flux lines naturally "prefer" to enter the ferrite horizontally. This behavior effectively utilizes the ferrite's magnetic properties, providing a more efficient pathway for energy transfer and offering more spatial flexibility to charge the vehicle .

In the VC configuration at figure 13, we have five receiver coils that loop over the ferromagnetic core. Each coil is connected to the same type of circuit as in the DDQ configuration.

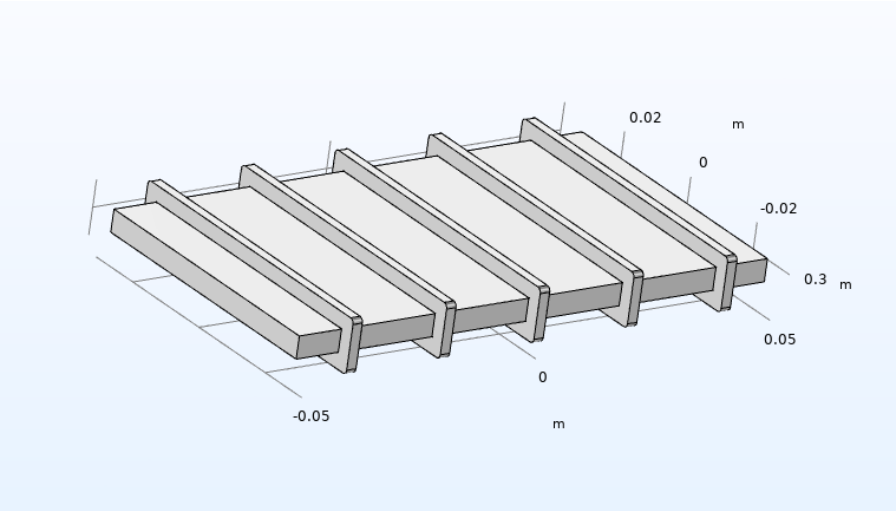

Figure 13-the new proposed VC configuration

Methodology

The goal of this work is to study the novel VC design, compare its performances to the DDQ design, and prove its superiority. To conduct this work, we operated on two complementary channels: simulations and physical measurements. In the simulation path, our initial focus was to study the the magnetic field distribution, ensuring that the VC successfully directs the field lines into the ferrite's cross section for achieving good field line concentration. Next, we mounted coils on the ferrite to calculate the induced voltage, which provided a basis for optimizing the system's energy transfer. Finally, we refined the coil's design to achieve the shape used in the current configuration.

Simulations played a crucial role in this work. The full-scale model is exceedingly large, and due to practical limitations, we were unable to construct it with the resources available in the lab. Instead, for the full size model, we relied on simulations to analyze its performance. To further support our concept and validate the simulation results, we constructed and simulated smaller-scale models of both the VC and the DDQ configurations. These scaled-down versions allowed us to verify the feasibility and effectiveness of our design while ensuring that the simulation results are aligned with experimental outcomes.

Additionally Performing circuit simulations using LTspice to complement the electromagnetic analysis required careful adjustments due to the challenges posed by frequency splitting and mutual inductance. Frequency splitting occurs in strongly coupled systems, causing the resonance frequency to split into two distinct frequencies. This can lead to reduced efficiency if the system is not precisely tuned to operate at one of these new frequencies. Similarly,

mutual inductance, which varies depending on the relative positions of the coils, can disrupt the balance of the system and shift the resonance frequency.

To address these issues, we had to fine-tune the system parameters, such as the capacitance and inductance values, to maintain resonance and ensure efficient coupling between the transmitter and receiver. These adjustments were critical to achieving a stable and effective energy transfer system, as even minor deviations could result in significant performance losses or instability in the circuit.

In the physical construction phase, we accounted for several limitations in the laboratory, such as the size of the available ferrite. Therefore, the scaled-down model didn't have the best dimension proportions and served mainly to explore the agreements and differences between the simulation and experiment. We designed a custom 3D-printed model to securely hold the entire configuration and allow for relative motion and positioning of the transmitter-receiver arrays. For the coils, we created a precise template to ensure they matched the dimensions and specifications used in the simulations as closely as possible.

Naturally, during the construction of the system, the components cannot be positioned with 100% accuracy as they are in the simulations. This can lead to slight deviations in the results between the experimental and simulated models. However, despite these differences, the overall behavior of the graphs remains consistent, and the results are similar, validating the reliability of the simulations in representing the system's performance.

The electronic circuits were built with selected components to fit most the simulation parameters. For conducting the experiment, we utilized a voltage generator and added an amplifier to provide sufficient voltage to activate the diodes. A Keysite Vector Network Analyzer (VNA) was employed to scan the frequency range and measure the response of the system, allowing us to evaluate its resonance characteristics and transmitted power.

In the following paragraphs, we will provide a detailed explanation of the methodology used in this work, including the steps taken in the design, simulation, construction, and testing phases.

Simulations

- COMSOL Multiphysics software tool has been utilized in this study. It is a versatile simulation software used for modelling and solving scientific and engineering problems. It employs the finite element method (FEM) [28] to numerically solve partial differential equations (PDE's) across various physical domains, such as electromagnetics, structural mechanics, acoustics, fluid dynamics, and chemical reactions. The software is designed to handle Multiphysics problems, where multiple physical phenomena interact within the same model [29].

We chose to use COMSOL Multiphysics for this work because it is a reliable and widely recognized simulation software used extensively around the world for various engineering and scientific applications. Additionally, we have significant experience working with this program, making it an ideal choice for conducting accurate and detailed simulations of our system.

To perform the simulations, we began by generating the required geometry for our system. Afterward, we defined the materials to be used, including copper for the coils, ferrite for magnetic guidance, and air for the surrounding volume. Next, we selected the appropriate simulation module, in this case, the Magnetic Fields (MF) module, which focuses on solving equations related to magnetic fields and currents within the system.

Once the physics were set, we defined the mesh for the model. The mesh determines the number of points where the Partial Differential Equations (PDEs) are solved. This can be adjusted to prioritize either accuracy (with a finer mesh and more points) or speed (with a coarser mesh and fewer points). It is crucial to strike the right balance here, as an insufficient number of points may lead to inaccurate solutions, while an excessive number can make the simulation unnecessarily slow.

We then specified whether the calculation would be stationary or time-dependent, depending on the nature of the simulation. COMSOL offers a variety of solution types to accommodate different scenarios. Finally, we defined the solver. In our case, we opted for an iterative solver, but there are other options, such as direct methods like LU decomposition or advanced techniques like Runge-Kutta for time-dependent problems. Each solver type influences the way the matrix equations are calculated and optimized for specific types of solutions. These thoughtful selections ensured the accuracy and efficiency of our simulations.

- LTspice software was used for the electric circuits simulations. It is a powerful and fast SPICE (Simulation Program with Integrated Circuit Emphasis) simulating software developed by Analog Devices. It is widely used in the industry for simulating analog electronic circuits. The software offers schematic capture and waveform viewing capabilities, making it a versatile tool for circuit design and analysis[30].

Our initial approach focused on creating the transmitting coils, as their design cannot be altered, and placing them alongside the ferrite in the simulated space. We applied voltage to the transmitting coils to evaluate whether the ferrite reached saturation. After confirming that the ferrite operated far from saturation, within its linear regime, we

proceeded to design the receiving coils and measured the voltage induced in them to assess the system's performance.

Subsequently, we adjusted the size of the coils to minimize their surface area while ensuring they adhered to the constraints imposed by the distance between the road and the vehicle. Once the design was finalized, we measured the self-inductance and mutual inductance of the system, as described in Equation 3. This measurement was conducted by ramping the current through the coils and recording the corresponding voltage. These values allowed us to validate the inductive properties of the system and make further optimizations to enhance its performance.

From the measured values of self-inductance and mutual inductance, along with the desired resonance frequency, we can determine the coupling coefficient K, as defined in Equation 4. Using these values, we calculate the appropriate capacitor sizes required to tune the system to the desired resonance frequency. This ensures optimal energy transfer by maintaining resonance in both the transmitting and receiving circuits.

Experimental

- A Vector Network Analyzer (VNA) by Keysite has been used for measuring the returning as well as the transmitted power through the DWPT coil layouts. It is an essential instrument used in RF (Radio Frequency) and microwave engineering to measure the electrical properties of networks, such as components or circuits, over a range of frequencies. It is widely used in the design, production, and testing of RF and microwave components, including antennas, amplifiers, filters, and cables. A VNA generates a known signal (stimulus) using its built-in signal source. This signal is then injected into the Device Under Test (DUT). The VNA has receivers that measure both the signal that is reflected from the DUT (due to impedance mismatches) and the signal that passes through the DUT (transmitted signal)[31].
- Pico Scope has been used to record the waveforms of the source, transmitter and receiver coils. It is a PC-based oscilloscope from Pico Technology that connects via USB or LPT ports, transforming a computer into a powerful oscilloscope and spectrum analyzer. The software supports advanced features such as real-time waveform display, FFT spectrum analysis, automated measurements, and various triggering options, including edge, window, and logic triggers. It includes high-performance specifications like bandwidths up to 1 GHz, sampling rates up to 5 GS/s, and buffer sizes up to 2 GS.

The setup is connected as follows: an AC voltage generator, operating at the resonance frequency, is connected to an amplifier. The output of the amplifier is then fed into the transmitting circuit. Energy is transferred via coupling from the transmitting circuit to the

receiving circuit. The configurations of both the transmitting and receiving circuits are illustrated in Figure 1, providing a visual representation of their structure and interconnection.

The receiving side contains the coils that couples with the transmitting side to capture the energy. Each inductor is paired with a capacitor to form a resonant circuit, tuned to the desired resonance frequency for maximum energy transfer. Following the resonant circuit, a rectification circuit is used to convert the alternating current (AC) into direct current (DC). Finally, the output of the rectification circuit is connected to a battery, where the energy is stored for later use.

After outlining the methodologies used for the simulations and experiments, we present the dimensions of the DDQ and VC configurations for both the simulated and laboratory models in the following table. This comparison highlights the key parameters and differences between the simulated designs and their physical counterparts, providing a clear reference for the setups used in this study.

It is important to once again note that while constructing the smaller models, we faced certain limitations due to restrictions on the available materials. These constraints influenced the design and construction process, requiring adjustments to the dimensions and components to align with what was feasible in the laboratory setting.

The primary purpose of building smaller models is not merely to rescale the full-size design but to validate the coherence between the simulation and experimental results. By ensuring that the outcomes of the simulations align with the experimental data, we can confidently rely on the simulation results without the need to construct massive and resource-intensive structures. This approach allows us to efficiently test and optimize the system's design principles while addressing practical constraints. The dimensions of both, full size and lab-scaled models are listed in table 1 below:

	VC large [cm]	VC lab [cm]	DDQ large [cm]	DDQ lab [cm]
Transmitter	Outer: 50x50 inner: 36.4 x 36.4 Thickness: 1	Outer: 5 x 5, inner: 4.8 x4.8 Thickness: 0.4	Outer: 50 x 50, inner: 36.4 x36.4 Thickness: 1	Outer: 5 x 5, inner: 4.8 x 4.8 Thickness: 0.4
Distance between centres of transmitting coils	75	6	75	6
Ferrite	125 x 40 x 6	10 x 0.44 x 5.6	125 x 250 x 1	10 x 0.44 x 5.6
Receiver	Outer: 10 x 50 Inner: 8 x 48 Height: 1	Outer: 1.05 x 6.2 Inner: 0.45 x 5.6 Height: 0.2	D: Outer 38 x 50 Inner: 29 x 41 Height: 1 Q: Outer: 50 x 50 Inner: 41 x 41 Height: 1	D: Outer: 3.8 x 5 Inner: 2.9 x 4.1 Height: 0.1 Q: Outer: 5 x 5 Inner: 3.95 x 3.95 Height: 0.1
Distance between receivers	25	2	DD: 0 Q: on top of DD coils centre	DD: 0 Q: on top of DD coils centre
Distance receivers from transmitting	30	3	30	3
Number of turns per coil	Transmitter: 11 Receiver: 10	Transmitter: 11 Receiver: 10	Transmitter: 11 D: 3.5 turns Q: 3.5 turns	Transmitter: 11 D: 3.5 turns Q: 3.5 turns

Table 1-dimensions of the DDQ and VC simulated and lab models

Results

As explained above, the main goals of this research are: 1. To prove the feasibility of the novel VC configuration suggested by our group. 2. To evaluate its energy transfer efficiency and compare it to the efficiency of the DDQ configuration. 3. To learn about the challenges related in further development and implementation of the VC concept. To achieve these goals, we begin with simulations of "real-size" transmitter and receiver coils, namely, coil dimensions that fit the actual implementation in the EV and in the road. Such dimensions have been obtained from Electreon Ltd., who provided us with the information about the state-of the-art DDQ receiver and transmitter coils being used in their projects. These dimensions are presented in table 1.

We begin with the calculations of the electromagnetic coupling coefficient, k, between all coils. For this purpose it is necessary to evaluate the self and mutual inductances between each pair of coils, thus we use the method described in the Methodology section . Table 2 lists the parameters obtained by applying this method [32] to the VC model configuration.

The self-inductance and mutual inductance were measured as described in the methodology section, using Equation 3. In the following tables, we present the mutual inductance values between all the coils, providing a detailed overview of the coupling characteristics within the system.

In Table 2, the mutual inductance values between VC1-5 and the transmitter, as well as among the VC coils themselves at the 0 position, are presented. The diagonal elements of the matrix represent the self-inductance of each coil. This matrix is inherently complex because it needs to be generated for each specific coil location, making the process computationally intensive and requiring precise measurements to capture the dynamic interactions accurately.

	VC1	VC2	VC3	VC4	VC5	Transmitter
VC1	1.79E-04	8.21E-05	5.59E-05	3.65E-05	1.79E-05	5.67E-06
VC2	8.21E-05	2.44E-04	1.21E-04	7.55E-05	3.65E-05	1.83E-05
VC3	5.59E-05	1.21E-04	2.62E-04	1.21E-04	5.59E-05	2.41E-05
VC4	3.65E-05	7.55E-05	1.21E-04	2.45E-04	8.20E-05	1.83E-05
VC5	1.79E-05	3.65E-05	5.59E-05	8.20E-05	1.79E-04	5.67E-06
Transmitter	5.67E-06	1.83E-05	2.41E-05	1.83E-05	5.67E-06	2.00E-04

Table 2-mutual inductance table of VC system at 0 position

As mentioned earlier, the mutual inductance matrix changes as the receiving side moves. To observe this effect, Table 3 presents the mutual inductance values at a position 20 cm away from the initial 0 position. This allows us to analyse how the interactions between the coils evolve with the displacement, offering insights into the dynamic behaviour of the system.

	VC1	VC2	VC3	VC4	VC5	Transmitter
VC1	1.79E-04	8.21E-05	5.59E-05	3.65E-05	1.79E-05	5.67E-06
VC2	8.25E-05	2.44E-04	1.21E-04	7.55E-05	3.65E-05	1.83E-05
VC3	5.64E-05	1.22E-04	2.62E-04	1.21E-04	5.59E-05	2.41E-05
VC4	3.68E-05	7.62E-05	1.22E-04	2.45E-04	8.20E-05	1.83E-05
VC5	1.81E-05	3.68E-05	5.63E-05	8.25E-05	1.79E-04	5.67E-06
Transmitter	1.22E-05	2.13E-05	1.83E-05	6.80E-06	1.94E-07	2.00E-04

Table 3-mutual inductance table of VC system at 20 position

The comparison between Table 2 and Table 3 reveals significant changes in the mutual inductance values across the VC system. These differences highlight the dynamic nature of the system as the receiver moves relative to the transmitter.

In particular, the mutual inductance between the transmitter and the individual VC coils shows noticeable variations. For example, the mutual inductance between the transmitter and VC1 increases from 5.67×10^{-6} to 1.22×10^{-5} , indicating a shift in the magnetic coupling strength due to the change in position. Similarly, the mutual inductance among the VC coils also changes significantly, reflecting the positional dependence of the system's coupling.

These changes underscore the complexity of designing and optimizing a dynamic wireless power transfer system. As the coils move, the interactions between them evolve, impacting the overall system performance. This behaviour must be carefully analysed and accounted for to ensure stable and efficient energy transfer under dynamic operating conditions.

The drastic changes in the mutual inductance not only affect the coupling coefficient, as shown in Equation 4, but also alter the resonance frequency of the system. These shifts can lead to complex multi-phenomena challenges, including frequency splitting, impedance mismatches, and reduced energy transfer efficiency.

Tables 4 and 5 present the coupling coefficients: Table 4 shows the coupling between the transmitter and the receivers and coupling among the receivers themselves, Table 5 shows the same but at different location. These tables clearly highlight the significant differences between the static and dynamic scenarios. In static conditions, the coupling coefficients remain constant, whereas in dynamic conditions, they vary with the relative positions of the coils, demonstrating the complexity and challenges of dynamic systems.

	VC1	VC2	VC3	VC4	VC5	Transmitter
VC1	100%	39.3%	25.8%	17.4%	10%	3%
VC2	39.3%	100%	47.7%	30.9%	17.4%	8.3%
VC3	25.8%	47.7%	100%	47.7%	25.8%	10.5%
VC4	17.4%	30.9%	47.7%	100%	39.2%	8.3%
VC5	10%	17.4%	25.8%	39.2%	100%	3%
Transmitter	3%	8.3%	10.5%	8.3%	3%	100%

Table 4-coupling table of VC system at 0 position

	VC1	VC2	VC3	VC4	VC5	Transmitter
VC1	100%	87.7%	63%	47.7%	37.6%	9%
VC2	87.7%	100%	84.6%	62%	48%	8.49%
VC3	63%	84.6%	100%	84.8%	63.5%	7.68%
VC4	47.7%	62%	84.8%	100%	88.6%	6.41%
VC5	37.6%	48%	63.5%	88.6%	100%	5%
Transmitter	9%	8.49%	7.68%	6.41%	5%	100%

Table 5-coupling table of VC system at 20 position

After examining the VC system, we can now compare it to the state-of-the-art DDQ configuration. The next two tables will present the mutual inductance matrices for the DDQ system at the 0 position and at the 20 cm position. These comparisons will provide a clear perspective on how the mutual inductance values differ between the two configurations under both static and dynamic conditions.

	DD	Q	Transmitter
DD	3.29E-04	5.75E-08	2.10E-05
Q	5.75E-08	2.22E-04	1.07E-09
Transmitter	2.10E-05	1.07E-09	2.00E-04

Table 6-mutual inductance table of VC system at 0 position

	DD	Q	Transmitter
DD	3.29E-04	1.75E-08	1.45E-05
Q	1.75E-08	2.22E-04	1.39E-05
Transmitter	1.45E-05	1.39E-05	2.00E-04

Table 7-mutual inductance table of VC system at 20 position

From these two tables, we observe that the mutual inductance between the DD coils and the transmitter remains relatively stable, as does the mutual inductance between the DD coils and the Q coil. However, the mutual inductance between the transmitter and the Q coil changes dramatically. This behaviour becomes even more apparent in the following two tables, which present the coupling coefficients. These tables provide a clearer visualization of how the interactions evolve under different positions, emphasizing the significant impact on the transmitter-Q coil coupling.

	DD	Q	Transmitter
DD	100%	0.0213%	8.19%
Q	0.0213%	100%	0.0005%
Transmitter	8.19%	0.0005%	100%

Table 8-coupling table of DDQ system at 0 position

	DD	Q	Transmitter
DD	100%	0.00647%	5.66%
Q	0.00647%	100%	6.60%
Transmitter	5.66%	6.60%	100%

Table 9-coupling table of DDQ system at 20 position

The performance evaluation of the full-scale DDQ and VC configurations reveals critical insights into the efficiency and practicality of each system. Both configurations were subjected to rigorous testing to measure their energy transfer capabilities and overall effectiveness in real-world conditions. The following sections present a detailed comparison of the two systems, highlighting their respective strengths and areas for improvement. After discussing the results from the full-scale models, we will delve into the findings from smaller-scale models, which were constructed and tested in the laboratory to further validate our simulations and theoretical predictions.

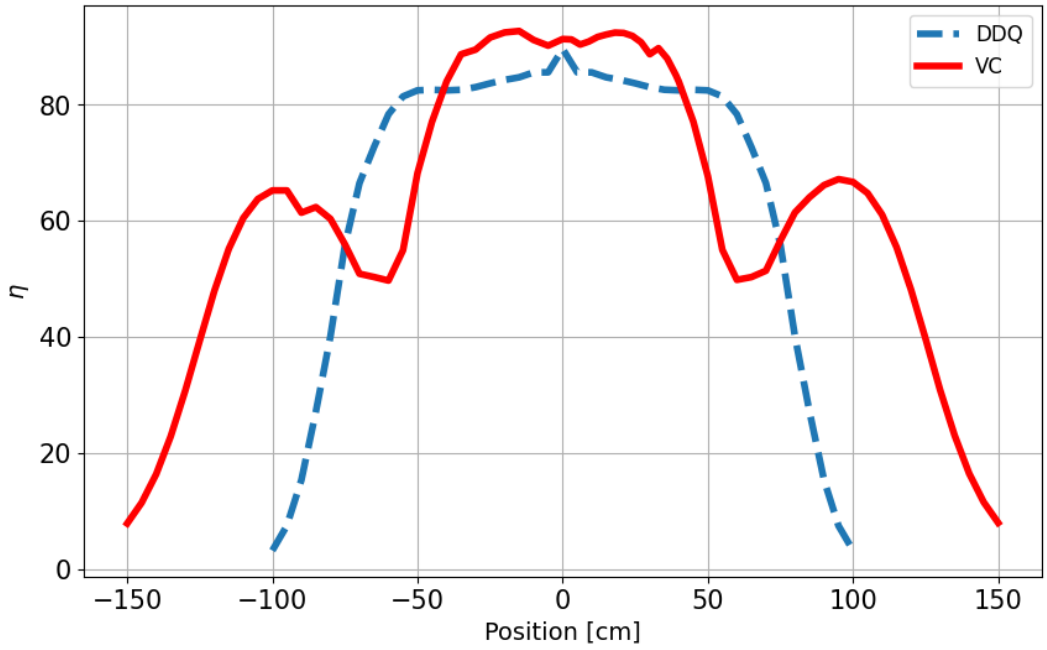

Figure 14- efficiency vs location of large DDQ and VC configurations

The efficiency of the DDQ configuration which can be seen at figure 14 reaches a maximum of around 85%. The efficiency remains nearly constant, at approximately 80%, between the positions of -50 cm to 50 cm. Beyond these points, the efficiency decreases significantly over the next 50 cm on each side, eventually dropping to nearly 0%. This behaviour indicates that the charging by the DDQ receiver is active over a distance of up 2 meters. However, most

efficient charging occurs within the central 1 meter of this range. This implies that while the system can provide continuous charging across a 2-meter span, optimal energy transfer is concentrated within the middle meter.

In the VC configuration, the maximum efficiency reaches approximately 93%. The graph reveals four distinct peaks: two central peaks reaching 93% efficiency, and two edge peaks reaching 66% efficiency The most efficient charging path is between -40 cm and 40 cm, where energy is transferred to the battery at an efficiency that exceeds 85%. Also seen here, are significant efficiency regions from -110 cm to -70 cm and from 70 cm to 110 cm, although these are less efficient compared to the central region. Beyond these points, the efficiency declines, reaching nearly 0% at -150 cm and 150 cm. This suggests that the VC system provides efficient energy transfer over a broader range compared to the DDQ configuration. The highest efficiency is still concentrated around the central region, with substantial but lower efficiency zones extending towards the edges as we can see at figure 14.

It is evident that the VC configuration is significantly more efficient. The comparison clearly shows that the VC graph is both wider and higher, indicating superior energy transfer efficiency compared to the alternative configuration. Keeping in mind that the charging process continues anytime η is greater than zero, the area beneath the graph represents the total energy that can be transferred to the battery. Therefore, the VC configuration offers roughly 50% more energy transfer in a single pass above the transmitter.

After analysing and integrating the energy transfer curves, we determined that the VC configuration achieves over 50% more energy transfer each time it passes over the transmitting coils compared to the DDQ configuration. This significant improvement highlights the effectiveness of the VC design in enhancing energy transfer efficiency.

After obtaining the promising results for the VC configuration, we constructed and simulated smaller models, as mentioned in the previous chapters. Although these models a simple, proportional scaled down models, they still serve the purpose of comparing between the simulation and experimental results. As we will show next, the small models demonstrated a good agreement between the simulation and the experimental, supporting the reliability of simulation methods for further research. It suggests that simulation models can be trusted for predicting the performance of the full-scale systems under similar conditions.

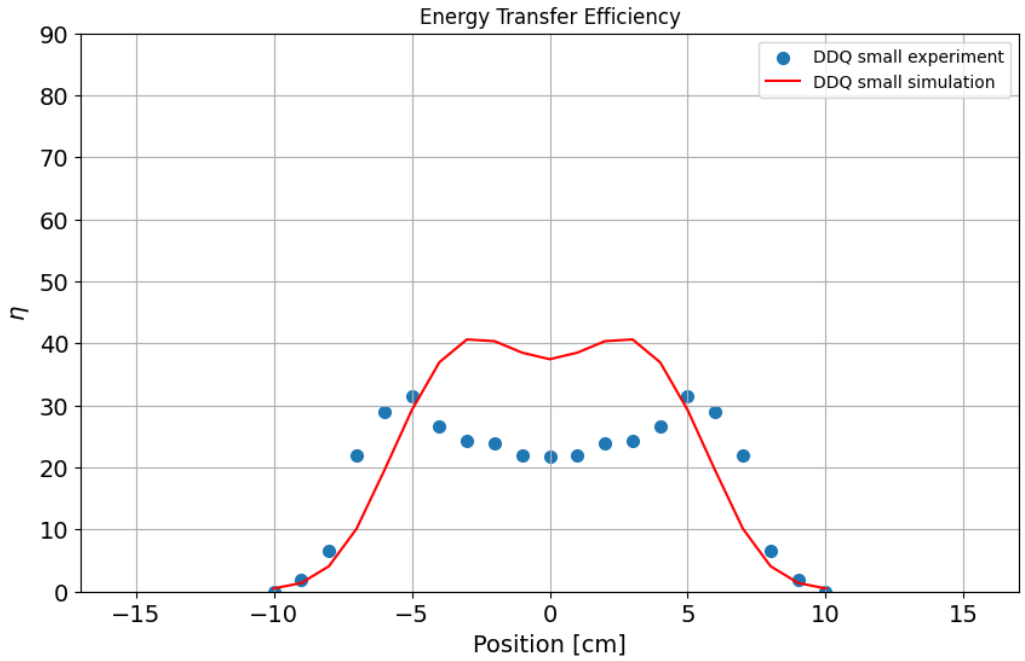

Figure 15-simulation and experiment efficiency graphs of small DDQ configuration

The small-scale model of the DDQ configuration deviated much from being a simple scale down from the large DDQ model described above. This is mainly because of the available ferrite plates at our reach, which dictated the dimensions of the DDQ coils that could fit beneath. Knowing that such a non-optimized model would result in far from optimal energy transfer efficiency values, we still chose to build, simulate and measure this model and compare between simulation and experimental results. The dimensions of the small DDQ model are listed in Table 1 above.

The efficiency graph obtained in the simulations of the small DDQ model is displayed in figure 15. It shows maximum efficiency of approximately 42%, far from the above 80% obtained for the large model. Notably, there is a small dip in the efficiency at the 0 cm position, which may be attributed to the distance between the DD coils. The most efficient charging occurs within the range of -4 cm to 4 cm. Beyond these points, the efficiency gradually decreases, reaching lower levels at distances of around 10 cm and -10 cm. This pattern suggests that optimal alignment is crucial for maintaining high efficiency, and even slight deviations can significantly impact the energy transfer capability.

In the experimental results for the small DDQ model, the maximum efficiency reached approximately 34%. This lower efficiency compared to the simulation, which showed a peak efficiency of 42%, may be attributed in part to real-world losses that were not fully accounted for in the simulation, such as losses in the wire and the ferrite material. The actual ferrite material was made of a stack of thin plates where for the simulations we used a ferrite bulk. Demagnetization effects in the thin plates as well as small gaps between these plates may also

contribute to increased losses and reduced efficiency. As the DDQ array moves from the centre, it experiences lower magnetic field intensities, the magnetization is lowered and so are the losses. Indeed, the simulations and experiment data better agree with each other at the marginal sections of the efficiency curves.

Next we examine the VC configuration. The efficiency graph of the small simulated VC configuration as we can see at figure 16 shows two peaks around 3 cm and -3 cm, with a noticeable dip at 0 cm. This dip is due to the spacing between the receiving coils. The efficiency decreases from these peaks until it reaches 0% at approximately ±15 cm. Along the way, there are smaller intermediate peaks, resulting from the summation of efficiency contributions from each coil.

To accurately determine the system's efficiency, we have to measure the efficiency of each coil in every position and sum all contributions correctly. For example, if we measure the entire system's efficiency at the 0 cm position, the second coil from the right, located at 2 cm, contributes to the efficiency at 2 cm rather than at 0 cm. This process ensures that the efficiency graph accurately reflects the contributions of each coil based on its location.

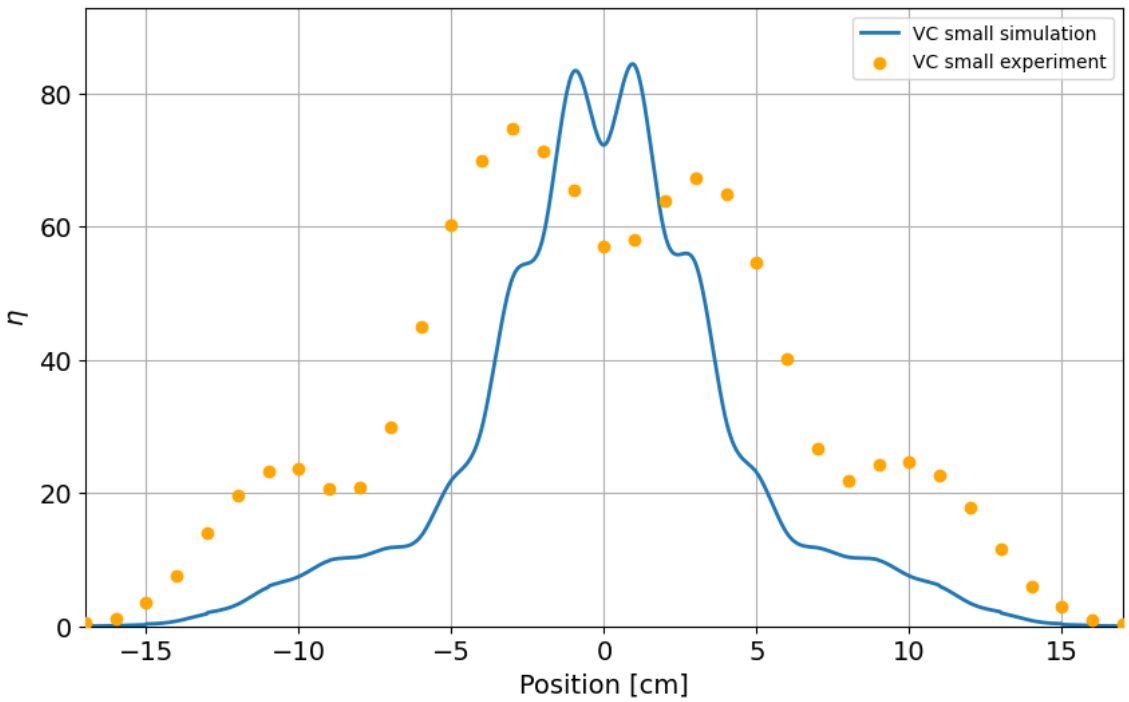

Figure 16- simulation and experiment efficiency graphs of small DDQ configuration

Figure 16 exhibits the experimental and simulated efficiency curves for the small VC configuration. The experimental data show nice qualitative and quantitative correlations with the simulation results. It feature two peaks at approximately 3 cm and -3 cm, along with a dip at 0 cm, similar to the simulation. The practical efficiency range spans from -16 cm to 16 cm, slightly broader than the simulated range of -15 cm to 15 cm.

There is a difference in the height of the peaks, which can be attributed to the challenges in constructing a highly precise system and again, to the actual ferrite characteristics And, of course, the demagnetization effect, similar to what occurs in the DDQ model. This construction variability also accounts for the difference in the span of the range. Despite these discrepancies, the overall match between the experimental and simulated data is fair, demonstrating the reliability and validity of the simulation in predicting real-world system performance.

VNA measurements

In the simulation, we obtained a graph depicting the relationship between frequency and power in decibels, providing a visual representation of the system's performance across a range of frequencies. Similarly, in the experimental setup, we utilized a Vector Network Analyzer (VNA) to achieve comparable results. The VNA is particularly effective in this context because it allows us to inject a wide range of frequencies into the system and measure the resulting power output, giving us detailed insights into the resonance characteristics of the coils.

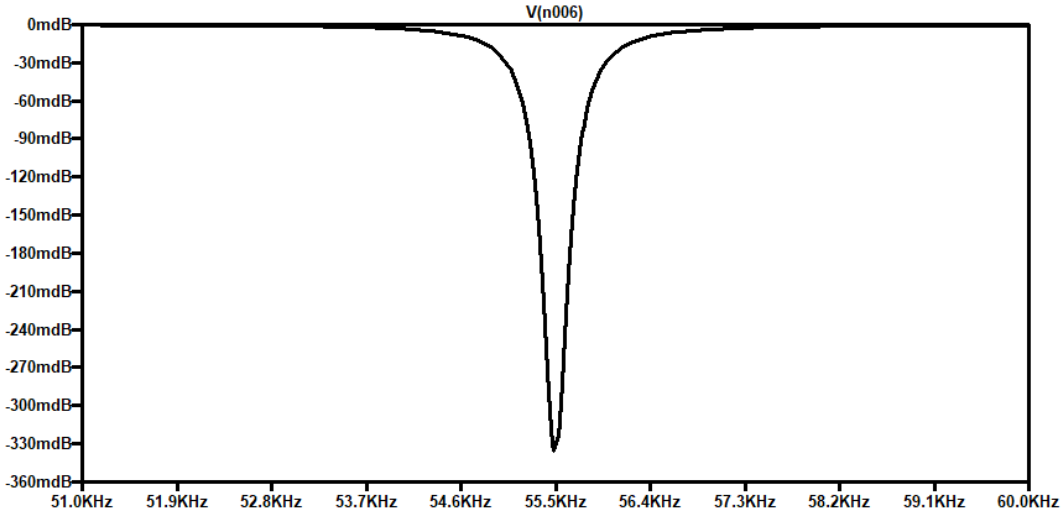

Figure 17-VC transmitting VNA measurement

To streamline the discussion and avoid redundancy, we will primarily focus on the transmission graph from the simulation of the VC configuration, as the remaining graphs exhibit similar patterns. In particular, the transmitting side of the graph will display a " dip " rather than a "peak" as observed in figure 17. This dip indicates the resonance frequency, where the system achieves maximum power transfer.

In the VC simulation, the resonance frequency is observed at approximately 55.5 kHz, which is consistent across all five receiver coils and at the transmitter as we can see at figure 17. This uniformity is expected in a controlled simulation environment where ideal conditions are assumed. However, when we moved to the experimental setup, the resonance frequencies showed some variation. The transmitting frequency was approximately 60 kHz, while coils 1, 2, 4, and 5 resonated around 56 kHz, and coil 3 resonated at 60 kHz. This discrepancy arises primarily because the transmitting side in the experiment had an inaccurate capacitance compared to the simulation, leading to shifts in the resonance frequencies. Additionally, significant mutual coupling between the receiving coils was observed, which further influenced their resonance frequencies. Initially, we aimed to set the entire system to resonate

at 85 kHz by carefully tuning each circuit. However, we quickly discovered that this approach was fraught with challenges due to the high nonlinearity of the system. In a highly nonlinear system like this, even minor variations, such as an extra wire loop or slight inaccuracies in the capacitors, can cause significant shifts in the resonance frequency of each coil. This made it difficult to achieve precise and consistent resonance across all coils in the VC configuration.

To address this problem of varying resonance frequencies, we can implement several strategies:

1. **Adjusting Capacitance**: One approach is to change the capacitance of each capacitor in the LC circuit on the receiving side. By altering the capacitance, we can directly influence the resonance frequency of each coil, bringing it closer to the desired target frequency.

2. **Modifying the Number of Coil Loops**: Another method is to change the number of loops in each receiver coil. This modification will alter the inductance of each coil, which in turn affects the resonance frequency. By carefully adjusting the coil's inductance, we can fine-tune the resonance frequency to match our desired specifications.

3. **Altering the Spacing Between Coils**: adjusting the space between the coils is an effective way to manage coupling effects. Increasing the distance between coils reduces the mutual coupling, thereby decreasing the interdependence of their resonance frequencies. This separation helps to stabilize the resonance frequencies across the system, aligning them more closely with the initial target frequency.

By employing these strategies, we can mitigate the challenges posed by the system's nonlinearity and improve the consistency of resonance frequencies across all coils, thereby enhancing the overall efficiency and performance of the system.

In contrast, the DDQ system was somewhat easier to manage regarding resonance frequencies. The DD coils and the Q coil exhibit very small mutual inductance, meaning they have minimal impact on each other's resonance frequencies. In the simulation, the transmitting side achieved a resonance frequency of approximately 86 kHz, with the receiving side's DD coils resonating at 87 kHz and the Q coil at 86 kHz. Similar to the VC system, our target was 85 kHz, but the simpler structure of the DDQ system, with only two receiving coils, resulted in less deviation from the target frequency compared to the more complex VC structure.

During the DDQ experiment, we again measured the resonance frequencies using a VNA. The results showed that the resonance frequency of the transmitter was around 80 kHz, while the DD coils also resonated at 80 kHz, and the Q coil resonated at 90 kHz. This shift in resonance frequencies can be attributed to the challenges in accurately achieving the desired capacitance values in the experimental setup. Even slight misalignments or inaccuracies can significantly impact the resonance frequency, particularly in a system as sensitive as this one.

In summary, while both the VC and DDQ configurations demonstrate the potential for high-efficiency power transfer, the VC configuration, despite its complexity and challenges, ultimately offers superior performance. The VC system′s multiple coils and significant mutual coupling present difficulties in maintaining consistent resonance frequencies, making it more challenging to manage. However, these same characteristics allow for a more efficient and flexible energy transfer system once properly tuned. On the other hand, the DDQ system, with its simpler configuration and lower mutual inductance, provides greater stability in maintaining target resonance frequencies, making it easier to manage in practice. Despite this, the VC configuration′s ability to achieve higher efficiency and better overall performance makes it a more advantageous choice, even when accounting for the additional challenges it presents.

Nonionizing radiation

Finally, in the VC configuration, windings are present also above the ferrite. Since radiation is often a topic of concern, especially when it comes to new technologies, we've looked into this issue.. People tend to worry about potential health risks associated with exposure to electromagnetic fields, particularly when they involve devices that operate close to the human body, like wireless power systems. This fear is not unfounded, as there is a general awareness of the effects of certain types of radiation, such as X-rays or ultraviolet light. However, it's important to recognize that we are constantly exposed to various forms of electromagnetic radiation in our daily lives—from Wi-Fi signals to cell phones, microwave ovens, and even natural sources like the Earth's magnetic field. Understanding the differences between these types of radiation and their effects on the human body is key to addressing these concerns. . In the case of wireless power transfer, the frequencies are low, similar to radio frequencies, and the levels of radiation are comparable to everyday sources, and stringent safety standards ensure that exposure remains well within safe limits. In our system, the radiation exposure experienced by individuals within the vehicle is comparable to the levels typically associated with household Wi-Fi networks. To ensure compliance with the radiation exposure standards established in Israel, we conducted measurements of the magnetic field strength at a distance of 1 cm above the receiver coil as we can see at figure 18. The results of these measurements demonstrated that the maximum magnetic field intensity recorded was 70 milligauss (mG), which remains below the Israeli regulatory limit of 75 mG and also below the ICNIRP limit [33] . As passenger's' body is situated well above 1 cm from the receiving coils, the radiation drops dramatically within the EV, This indicates that our wireless power transfer system operates within the safe boundaries set for radiation exposure, ensuring that occupants are not subjected to harmful levels of electromagnetic fields.

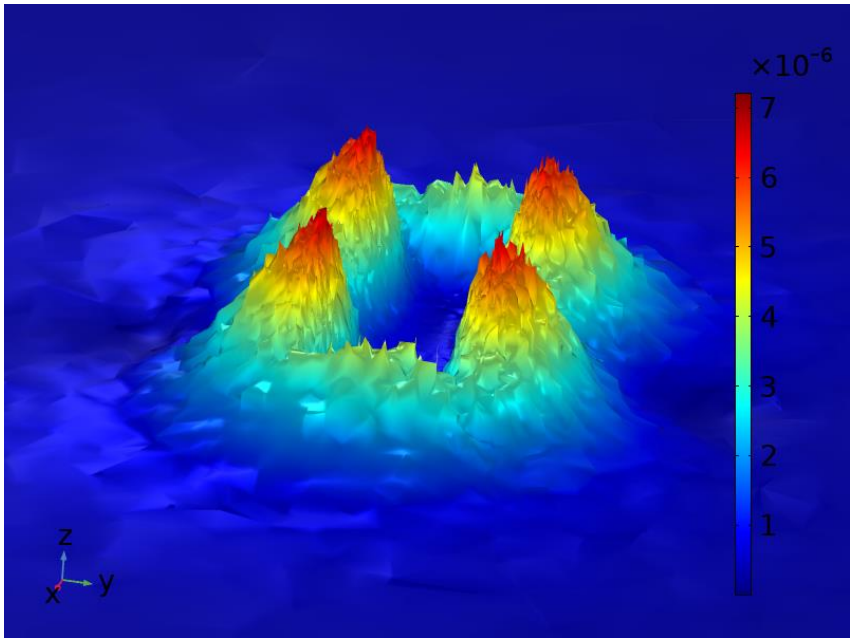

Figure 18-magnetic field [T] cross section 1 cm above the receiver system

Summary & Conclusions

This work introduces a new receiver coil configuration, the Vertical Coil (VC) design, for Dynamic Wireless Power Transfer (DWPT) systems used in charging electric vehicles. The VC design aims to improve energy transfer efficiency by using multiple vertically aligned coils wound around a ferrite core. This is in contrast to the conventional and commercially used DDQ receiver coils, which are horizontally oriented.
The novelty of the VC concept lies in its ability to collect more magnetic flux while keeping the cross section of the pickup coils small. This is achieved on one hand by the vertical positioning of the coils so that they better face the magnetic flux lines. On the other hand, the introduction of a ferrite core inside the coils, concentrates the flux within the coils thus overcomes the physical constrain of the clear space beneath the EV, so that energy transfer efficiency is reached even for reduced coil heights.

To prove the feasibility of the VC concept we have conducted simulations and experiments on both full-scale and small, bench-top models of the VC and DDQ designs. Their findings show that the VC configuration not only yields a higher peak efficiency when the receiver is positioned directly above the transmitter but also spans a larger range of efficient energy transfer.

Key benefits of the VC design:

- Higher peak efficiency: The VC design achieves approximately 93% peak efficiency compared to the DDQ's 85%.
- Wider range of efficiency: The VC design maintains efficient energy transfer over a broader range than the DDQ.
- Greater total energy transfer: The VC receiver can harvest over 50% more energy from the source during a full pass than the DDQ receiver.

Despite the success in proving the feasibility of the VC concept for DWPT, some difficulties and open questions have been raised in this work:

1. Simulation and experimental results are expected to better match. Although we have found a qualitative agreement between the two in the behaviour of the energy transfer efficiency during a pass over the transmitter, there are quantitative mismatches between the values. Near the center position, the simulation results in higher efficiency than the experimental, but at the margins of the efficiency curve the actual data wins. We attribute this discrepancy to the difference between the actual ferrite plates used in the physical model and the bulk used in the simulations. Further studies need to be performed to validate this assumption and narrow the gap between the simulations and "real life" data so that simulations could be fully trusted in further designs.

2. Nonlinear complex behavior is more pronounced in the VC design. The use of several coils sharing the same ferromagnetic core, exposes the system to increased inter-coupling between all coils and increased non-linearity. The system is now sensitive not only to its relative position between the transmitter and the receiver, but also to the local magnetization state of the core. Further research is required to thoroughly describe the non-linear nature of the design.
3. Resonance shift. The interplay between the vertical coils dynamically affects their mutual inductance and coupling and as a result shifts the resonance frequency from its pre-designed values. We continue to analyze the findings and to suggest ways to either correct the design or compensate for this shift dynamically.

We strongly believe that the VC design has the potential to significantly improve the performance of DWPT systems, contributing to the advancement of dynamic wireless power transfer technology and the EV industry.
A provisional patent for the VC concept has been submitted and initial steps to interest the relevant industry has been taken. This work has been submitted for publication in "IEEE Transactions on Industrial Electronics", a leading Q1 journal in the field. It is now under review. A copy of the submitted paper is attached here.

Future Research Directions

There are multiple ways to proceed with further research aimed at improving the efficiency and practicality of DWPT systems. Future studies can explore:

1. **Changing the number of turns in the coils**: By increasing or decreasing the number of turns, it may be possible to optimize the inductance and resonance frequency, potentially improving coupling efficiency over longer distances.

2. **Adjusting the number of receiving coils**: Investigating how varying the number of receiver coils affects energy transfer efficiency could provide insights into maximizing power delivery, especially for larger or faster-moving vehicles.

3. **Modifying the size of the coils**: Changing the dimensions of the receiving coils could lead to a more efficient magnetic field distribution, improving the range and power transfer capabilities of the system.

4. **Altering the spacing between coils**: The distance between the receiving coils plays a crucial role in coupling efficiency. Further research could focus on optimizing this spacing to achieve better performance over varying air gaps and road conditions.

5. **Incorporating superconducting coils**: Using superconducting materials in the transmitting and receiving coils could drastically reduce resistance, increasing the overall system efficiency as we can see at [34][35][36]. Superconducting coils could also allow for higher power transmission without significant energy loss, making DWPT systems more practical for real-world applications.

Each of these research directions offers a path to refine the current systems and push DWPT technology towards becoming a more reliable and efficient solution for wireless electric vehicle charging.

Bibliography

[1] K. Chen and J. F. Pan, "Dynamic Wireless Power Transfer System for Electric Vehicles - Development and Challenges," in *2022 IEEE 9th International Conference on Power Electronics Systems and Applications (PESA)*, IEEE, Sep. 2022, pp. 1–11. doi: 10.1109/PESA55501.2022.10038419.

[2] TOI STAFF, "1,200 miles: Israeli startup Electreon sets record for longest drive by electric car."

[3] JARRYD NEVES, "America's First Wireless Charging Road Opens In Detroit," 2023.

[4] "Electreon's Wireless Electric Road Technology Sets a New World Record: The Longest Distance Ever Driven By A Passenger Electric Vehicle (EV) For Over 100 Hours, Solving the Most Acute Challenges of EV Adoption," *https://electreon.com/articles/electreons-wireless-electric-road-technology-sets-a-new-world-record-the-longest-distance-ever-driven-by-a-passenger-electric-vehicle-ev-for-over-100-hours-solving-the-most-acute-challenges-of-e*.

[5] I. Garofy, A. Roitman, Y. Nikulshin, and S. Wolfus, "Vertical Receiver Coils for Improved Energy Transfer Efficiency in Dynamic Wireless Charging of Electric Vehicles." Nov.2024 . *IEEE Transactions on Industrial Electronics. Submitted.*

[6] K. Ünal, G. Bal, and S. Öncü, "Wireless Power Transfer," in *Power Electronics Handbook*, Elsevier, 2024, pp. 759–778. doi: 10.1016/B978-0-323-99216-9.00007-X.

[7] O. Shimizu, S. Nagai, T. Fujita, and H. Fujimoto, "Potential for CO2 Reduction by Dynamic Wireless Power Transfer for Passenger Vehicles in Japan," *Energies (Basel)*, vol. 13, no. 13, p. 3342, Jun. 2020, doi: 10.3390/en13133342.

[8] P. Lazzeroni, V. Cirimele, and A. Canova, "Economic and environmental sustainability of Dynamic Wireless Power Transfer for electric vehicles supporting reduction of local air pollutant emissions," *Renewable and Sustainable Energy Reviews*, vol. 138, p. 110537, Mar. 2021, doi: 10.1016/j.rser.2020.110537.

[9] M. Redelbach, M. Klötzke, and H. E. Friedrich, "Impact of lightweight design on energy consumption and cost effectiveness of alternative powertrain concepts."

[10] K. Qian, C. Zhou, M. Allan, and Y. Yuan, "Modeling of Load Demand Due to EV Battery Charging in Distribution Systems," *IEEE Transactions on Power Systems*, vol. 26, no. 2, pp. 802–810, May 2011, doi: 10.1109/TPWRS.2010.2057456.

[11] J. C. Gómez and M. M. Morcos, "Impact of EV battery chargers on the power quality of distribution systems," *IEEE Transactions on Power Delivery*, vol. 18, no. 3, pp. 975–981, Jul. 2003, doi: 10.1109/TPWRD.2003.813873.

[12] N. A. Zakaria *et al.*, "A Computational Study on the Magnetic Resonance Coupling Technique for Wireless Power Transfer," *MATEC Web of Conferences*, vol. 140, p. 01025, Dec. 2017, doi: 10.1051/matecconf/201714001025.

[13] M. A. Habibi, C. Fall, E. Setiawan, I. Hodaka, Wijono, and R. N. Hasanah, "The use of mathematics and electric circuit simulator software in the learning process of wireless power transfer for electrical engineering students," in *AIP Conference Proceedings*, American Institute of Physics Inc., Sep. 2017. doi: 10.1063/1.5003500.

[14] A. Ali *et al.*, "A Comprehensive Review of Midrange Wireless Power Transfer Using Dielectric Resonators," *Int J Antennas Propag*, vol. 2021, pp. 1–14, Jul. 2021, doi: 10.1155/2021/5493013.

[15] Md. A. Yousuf, T. K. Das, Md. E. Khallil, N. A. Ab. Aziz, Md. J. Rana, and S. Hossain, "Comparison Study of Inductive Coupling and Magnetic Resonant Coupling Method for Wireless Power Transmission of Electric Vehicles," in *2021 2nd International Conference on Robotics, Electrical and Signal Processing Techniques (ICREST)*, IEEE, Jan. 2021, pp. 737–741. doi: 10.1109/ICREST51555.2021.9331096.

[16] "parameters of ferrite ." Accessed: Oct. 08, 2024. [Online]. Available: https://www.laird.com/products/inductive-components-emc-components-and-ferrite-cores/ferrite-plates-and-disks/mp-series/mp3940-0m0

[17] G. J. Aubrecht, D. M. Scott, K. Tanaka, and R. Torgerson, "Resonance splitting," *Ann Phys (N Y)*, vol. 68, no. 2, pp. 499–508, Dec. 1971, doi: 10.1016/0003-4916(71)90132-1.

[18] S Lee, "On-line electric vehicle using inductive power transfer system," *Energy Conversion Congress and Exposition*, pp. 1598–1601, 2010.

[19] Y D Ko and Y J Jang, "The optimal system design of the online electric vehicle utilizing wireless power transmission technology," *IEEE Transactions on Intelligent Transportation Systems* , pp. 1255–1265, 2013.

[20] N P Suh, "Design of on-line electric vehicle (OLEV)," *Global product development*, pp. 3–8, 2011.

[21] J. Shin *et al.*, "Design and Implementation of Shaped Magnetic-Resonance-Based Wireless Power Transfer System for Roadway-Powered Moving Electric Vehicles," *IEEE Transactions on Industrial Electronics*, vol. 61, no. 3, pp. 1179–1192, Mar. 2014, doi: 10.1109/TIE.2013.2258294.

[22] S Y Choi, "Ultraslim S-type power supply rails for road- way-powered electric vehicles," *IEEE Transactions on Power Electronics 30.11*, pp. 6456–6468, 2015.

[23] J Huh, "Narrow-width inductive power transfer system for online electrical vehicles," *IEEE Transactions on Power Electronics 26.12*, pp. 3666–3679, 2011.

[24] N. K. Trung and N. T. Diep, "A Maximum Transfer Efficiency Tracking Method for Dynamic Wireless Charging Systems of Electric Vehicles," *Journal of Electrical and Computer Engineering*, vol. 2021, pp. 1–10, Nov. 2021, doi: 10.1155/2021/5562125.

[25] Bareli Sahar, "Effect of Coil Configuration on Dynamic Wireless Power Transfer for Electric Vehicle Applications," 2021.

[26] N. Prosen, J. Domajnko, and M. Milanovič, "Wireless Power Transfer Using Double DD Coils," *Electronics (Basel)*, vol. 10, no. 20, p. 2528, Oct. 2021, doi: 10.3390/electronics10202528.

[27] Z. Deng *et al.*, "Design of a 60kW EV Dynamic Wireless Power Transfer System with Dual Transmitters and Dual Receivers," *IEEE J Emerg Sel Top Power Electron*, pp. 1–1, 2023, doi: 10.1109/JESTPE.2023.3301579.

[28] "The Finite Element Method: Its Basis and Fundamentals," in *The Finite Element Method: its Basis and Fundamentals*, Elsevier, 2013, p. i. doi: 10.1016/B978-1-85617-633-0.00019-8.

[29] "COMSOL Multiphysics." Accessed: Oct. 28, 2024. [Online]. Available: COMSOL AB. COMSOL Multiphysics® (Version 5.6) [software]. Stockholm, Sweden: COMSOL AB; 2020. Available from: https://www.comsol.com

[30] "LTspice." Accessed: Oct. 28, 2024. [Online]. Available: Analog Devices, Inc. LTspice® XVII (Version 17.0) [software]. Wilmington, MA: Analog Devices; 2018. Available from: https://www.analog.com/en/design-center/design-tools-and-calculators/ltspice-simulator.html

[31] "KEYSIGHT ." Accessed: Oct. 28, 2024. [Online]. Available: https://www.keysight.com/us/en/products/network-analyzers/streamline-series-usb-vector-network-analyzers.html

[32] J. Linden, Y. Nikulshin, S. Wolfus, H. Rumbak, O. Ezer, and Y. Yeshurun, "Method for calculating coupling coefficients in dynamic energy transfer for electric vehicles," in *2017 Electric Vehicles International Conference (EV)*, IEEE, Oct. 2017, pp. 1–4. doi: 10.1109/EV.2017.8242111.

[33] "GUIDELINES FOR LIMITING EXPOSURE TO TIME-VARYING ELECTRIC AND MAGNETIC FIELDS (1 Hz TO 100 kHz)," *Health Phys*, vol. 99, no. 6, pp. 818–836, Dec. 2010, doi: 10.1097/HP.0b013e3181f06c86.

[34] C. Utschick, C. Som, J. Souc, V. Grose, F. Gomory, and R. Gross, "Superconducting Wireless Power Transfer Beyond 5 kW at High Power Density for Industrial Applications and Fast Battery Charging," *IEEE Transactions on Applied Superconductivity*, vol. 31, no. 3, pp. 1–10, Apr. 2021, doi: 10.1109/TASC.2021.3056195.

[35] R. Lyu, W. Liu, Q. Li, and K. T. Chau, "Overview of superconducting wireless power transfer," *Energy Reports*, vol. 12, pp. 4055–4075, Dec. 2024, doi: 10.1016/j.egyr.2024.09.067.

[36] N. Oshimoto, K. Sakuma, and N. Sekiya, "Improvement in Power Transmission Efficiency of Wireless Power Transfer System Using Superconducting Intermediate Coil," *IEEE Transactions on Applied Superconductivity*, vol. 33, no. 5, pp. 1–4, Aug. 2023, doi: 10.1109/TASC.2023.3256342.

תקציר

עבודה זו מציגה תצורה חדשה של סלילי מקלט עבור מערכות העברת אנרגיה אלחוטית דינמית (Dynamic Wireless Power Transfer (DWPT, המשמשות לטעינת כלי רכב חשמליים במהלך התנועה וללא צורך בעצירה. אנו מציעים תצורת סלילים אנכיים (Vertical Coils (VC המלופפים סביב ליבה מגנטית מסוג פריט (ferrite) באופן המאונך לכיוון התנועה ולכביש. זאת בניגוד לסלילי המקלט הקונבנציונליים והמסחריים המכוונים אופקית. החידוש ברעיון ה- VC טמון ביכולתו לאסוף יותר שטף מגנטי תוך שמירה על שטח חתך קטן בסלילים. הישג זה מתקבל על ידי מיקומם האנכי של הסלילים, כך שהם אוספים טוב יותר קווי שטף המגנטי. בנוסף, הכנסת ליבת פריט בתוך הסלילים מרכזת את השטף בתוך הסלילים ובכך מתגברת על המגבלה הפיזית של החלל הפנוי מתחת לרכב החשמלי, כך שיעילות העברת האנרגיה מושגת גם עבור גובה סליל מופחת.

כדי להוכיח את ההיתכנות של רעיון ה-VC ערכנו סימולציות וניסויים הן בקנה מידה מלא והן בדגמים קטנים, של תצורת VC והמתחרה (מכונה בשם DDQ). הממצאים מראים כי תצורת VC לא רק מניבה יעילות שיא גבוהה יותר כאשר המקלט ממוקם ישירות מעל המשדר, אלא גם מאפשרת קליטה המשתרעת על פני טווח גדול יותר של העברת אנרגיה יעילה.

היתרונות העיקריים של תכנון VC:

- **יעילות שיא גבוהה יותר:** תצורת VC משיגה יעילות שיא של כ-93% בהשוואה ל-85% של ה-DDQ.
- **טווח רחב יותר של יעילות:** תכנון VC מאפשר העברת אנרגיה יעילה בטווח רחב יותר מאשר DDQ.
- **העברת אנרגיה כוללת גדולה יותר:** מקלט VC יכול לקצור מעל 50% יותר אנרגיה מהמקור במהלך מעבר מלא מאשר מקלט DDQ.

למרות ההצלחה בהוכחת ההיתכנות של רעיון ה- VC עבור DWPT, כמה קשיים ושאלות פתוחות הועלו בעבודה זו:

א. **תוצאות הסימולציה והניסוי צפויות להתאים טוב יותר**. למרות שמצאנו הסכמה איכותית בין השניים בהתנהגות יעילות העברת האנרגיה במהלך מעבר מעל המשדר, קיימות אי התאמות כמותיות בין הערכים. בסמוך למיקום המרכזי, הסימולציה מביאה ליעילות גבוהה יותר מהניסוי, אך בשולי עקומת היעילות הנתונים בפועל מנצחים. אנו מייחסים פער זה להבדל בין לוחות הפריט בפועל המשמשים במודל הפיזיקלי לבין הרוב המשמש בסימולציות.

ב. **התנהגות מורכבת לא ליניארית בולטת יותר בתכנון VC**. השימוש במספר סלילים החולקים את אותה ליבה פרומגנטית, חושף את המערכת לצימוד הדדי מוגבר בין כל הסלילים ולאי-ליניאריות מוגברת. המערכת רגישה כיום לא רק למיקומה היחסי בין המשדר למקלט, אלא גם למצב המגנטיזציה המקומי של הליבה.

ג. **שינוי תדרי התהודה**. יחסי הגומלין בין הסלילים האנכיים משפיעים באופן דינמי על ההשראות העצמית וההדדית שלהם וכתוצאה מכך מזיזים את תדר התהודה מערכיו שתוכננו מראש.

קבוצת המחקר שלנו ממשיכה בעבודה כדי להתמודד עם הנקודות הללו, להשיג הבנה עמוקה יותר ולשפר עוד את הביצועים. אנו מאמינים כי לתכנון VC יש פוטנציאל לשפר באופן משמעותי את הביצועים של מערכות DWPT, ולתרום לקידום טכנולוגיית העברת כוח אלחוטית דינמית ותעשיית הרכב החשמלי.
הוגשה בקשה מקדמית לפטנט זמני ונשלח מאמר מדעי לפרסום.

עבודה זו נעשתה בהדרכתו של ד״ר שוקי וולפוס.

המחלקה לפיזיקה, אוניברסיטת בר אילן.

אוניברסיטת בר אילן

אופטימיזציה של סלילי שידור וקליטה לשיפור יעילות העברת האנרגיה בטעינה אלחוטית דינמית ברכבים חשמליים

איתי ג׳רופי

עבודה זו מוגשת כחלק מהדרישות לשם קבלת תואר מוסמך במחלקה לפיסיקה של אוניברסיטת בר אילן

רמת גן תשפ״ה